months. The absence of lamivudine resistance was defined by no detection of the rtM204V/I substitution as measured by the PCR–enzyme linked minisequence assay (ELMA) (Sumitomo Metal Industries) [20] for 33 patients, or by the lack of virological breakthrough as judged by more than 1 log increment in HBV DNA from the nadir for the remaining 11 patients. All of the 44 patients switched to 0.5 mg/day of entecavir administration. After the beginning of entecavir treatment, liver function tests and HBV markers were measured at 1- to 2-month intervals. When virological breakthrough was observed during follow-up, entecavir-resistance-associated mutations were examined by means of a PCR-direct sequencing method. The follow-up period of entecavir treatment ranged from 10 to 23 (median 20) months.

Baseline characteristics of the patients

At the commencement of switching treatment to entecavir, the 28 males and 16 females were aged 33–79 (median 59) years. Seventeen patients (39%) tested positive for hepatitis B e antigen (HBeAg), and antibody against HBeAg (anti-HBe) developed in all of the 27 HBeAg-negative patients. Among the 27 HBeAg-negative patients, four achieved HBeAg clearance during the preceding lamivudine treatment. HBV DNA at baseline varied among patients from <2.6 to 5.2 logcopies/ml. The baseline ALT ranged from 11 to 78 (median 25) IU/l. Regarding the liver diseases of the patients, 27 (61%) showed features of chronic hepatitis, 11 (25%) of liver cirrhosis and six (14%) of hepatocellular carcinoma (HCC) according to liver biopsy and/or abdominal imaging procedures. HBV genotype was examined for 14 patients, and all of them had HBV genotype C, the most predominant genotype in Japan. Informed consent was obtained from all patients.

Serological and virological markers of HBV

HBsAg, HBeAg and anti-HBe were determined by chemiluminescent immunoassay. HBV DNA was measured by the PCR-based method (Amplicor HBV monitor, Roche Diagnostics) whose lower detection limit is 2.6 logcopies/ml. Lamivudine-resistant rtM204V/I substitution was examined by the PCR–ELMA method (Sumitomo Metal Industries) (20), which is capable of detecting the mutant virus in a mixed viral population if it is present at more than 10% of the total population. The entecavir-resistance-associated substitutions and HBV genotype were determined by a PCR-direct sequencing method. As for oligonucleotide primers for PCR reaction, the outer primer sets were BF5 (5′-AAG AGA CAG TCA TCC TCA GG-3′, nt 3183–3202) and BR1s (5′-AAA AAG TTG CAT GGT GCT GG-3′, nt 1825–1806), and the inner primer sets were BF6 (5′-CCT CCA ATT TGT CCT GGC TA-3′, nt 350–369) and BR8 (5′-TTG CGT CAG CAA ACA CTT GG-3′, nt 1195–1176). After DNA extraction, the DNA sample was subjected to the PCR reaction for 35 cycles (denaturation at 94°C for 1 min, annealing at 55°C for 1 min and extension at 72°C for 2 min) using the inner primer set, followed by a final extension at 72°C for 10 min. If amplification was not successful by the single PCR reaction, the nested PCR was conducted; the first round PCR was done using the outer primer sets for 35 cycles, and the aliquot of the product was used for the second round PCR for 30 cycles using inner primer sets. All sequencing reactions of the PCR products were carried out using the BigDye Terminater Ver. 3.1 Cycle Sequencing Kit, and 3100 or 3730 Genetic Analyzer (Applied Biosystems), which allowed determination of the amino acid sequences of rt85-344. For determining the HBV genotype, nucleotide sequences obtained in each of the patients were aligned along with representative HBV strains of genotype A–H, and a phylogenetic tree was constructed in the homepage of DNA Data Bank of Japan (http://www.ddbj.nig.ac.jp).

Statistical analysis

Statistical analysis for group comparison was performed by Fisher's exact probability test and Mann–Whitney's non-parametric U test using the SPSS version 15.0J software (SPSS Inc, Chicago, IL). A p value of less than <.05 was considered to be significant.

Results

Classification of patients who underwent lamivudine-to-entecavir switching treatment according to baseline HBV DNA

The 44 CH-B patients who underwent the switching treatment from lamivudine to entecavir were first classified according to their baseline HBV DNA at the commencement of entecavir administration. HBV DNA was not detectable (<2.6 logcopies/ml) in 31 patients (70%) at baseline. Seven patients (16%) had baseline HBV DNA of 2.6–<4.0 logcopies/ml. In the remaining six patients (14%), the baseline HBV DNA was ≥4.0 logcopies/ml. When patient clinical characteristics were compared among the three patient groups (Table 1), nine (29%) of the 31 patients with baseline HBV DNA <2.6 copies/ml tested positive for HBeAg at the commencement of switching treatment to entecavir, compared with five of the six (83%) patients with baseline HBV DNA ≥4.0 copies/ml ($p < .05$). Gender ratio, age, ALT at baseline, liver disease, duration of the preceding lamivudine treatment and

Table 1 Patient clinical characteristics and the therapeutic efficacy in 44 CH-B patients in relation to their baseline HBV DNA

	Baseline HBV DNA		
	<2.6 logcopies/ml ($n = 31$)	2.6–<4.0 logcopies/ml ($n = 7$)	≥4.0 logcopies/ml ($n = 6$)
At the commencement of switching treatment to entecavir			
Gender (male/female)	19/12	5/2	4/2
Age (years)	60 (35–79)[a]	65 (41–69)	55 (33–65)
HBeAg (positive/negative)	9/22	3/4	5/1[b]
HBV DNA (logcopies/ml)	<2.6	3.1 (2.6–3.6)[c]	4.6 (4.0–5.2)[c,d]
rtM204V/I mutation (absence/NT)	23/8	5/2	5/1
ALT (IU/l)	25 (11–64)	31 (13–46)	20 (17–78)
Chronic hepatitis/cirrhosis/HCC	19/7/5	4/2/1	4/2/0
Follow-up period of entecavir treatment (months)	19 (10–23)	19 (10–22)	20 (16–22)
The rate of undetectable HBV DNA level during follow-up	31 (100%)	7 (100%)	3 (50%)[c]
Emergence of entecavir-resistance during follow-up	0 (0%)	0 (0%)	1 (17%)
At the commencement of preceding lamivudine treatment			
HBeAg (positive/negative)	12/19	4/3	5/1
HBV DNA (logcopies/ml)	6.5 (4.3–7.6‹)	6.6 (6.2–7.6‹)	7.6‹ (5.9–7.6‹)
Duration of preceding lamivudine treatment (months)	15 (6–73)	10 (7–42)	9 (8–32)

NT not tested

[a] Values are expressed as median (range)

[b] $p < .05$ versus baseline HBV DNA <2.6 logcopies/ml group

[c] $p < .01$ versus baseline HBV DNA <2.6 logcopies/ml group

[d] $p < .01$ versus baseline HBV DNA of 2.6–<4.0 logcopies/ml group

follow-up period of entecavir treatment did not differ among the three groups. Also, there was no significant difference in HBV DNA and the frequency of positive HBeAg at the commencement of preceding lamivudine treatment among them.

Antiviral efficacy and drug resistance in lamivudine-to-entecavir switching treatment in relation to baseline HBV DNA

Next, we investigated serial changes in HBV DNA after the switch from lamivudine to entecavir treatment in CH-B patients in relation to the baseline HBV DNA. All 31 patients with baseline HBV DNA <2.6 logcopies/ml maintained undetectable HBV DNA during the follow-up period of entecavir treatment. Figure 1 shows the longitudinal evaluation of HBV DNA during the switching treatment to entecavir in patients with a detectable level of baseline HBV DNA. In patients having baseline HBV DNA of 2.6–<4.0 logcopies/ml (Fig. 1a), all of the seven patients achieved sustained undetectable HBV DNA during follow-up, although HBV DNA was transiently detected in one patient. As for patients having baseline HBV DNA ≥4.0 logcopies/ml (Fig. 1b), three (50%) of the six patients achieved sustained undetectable HBV DNA during follow-up. In two patients, HBV DNA was not cleared entirely, but declined to 2.9 and 2.7 logcopies/ml at month 18, respectively. In sequencing analysis at that time, the former patient had the lamivudine-resistant rtM204I substitution, although it was not detected by the PCR–ELMA assay at the start of entecavir treatment. The latter patient had no drug resistance-associated substitutions. In the sixth patient, HBV DNA decreased initially, but virological breakthrough was seen at month 15. The entecavir-resistant virus was detected after virological breakthrough. The detailed disease course of the entecavir-resistant patient is described below. As for the relationship of baseline HBV DNA to the frequency of undetectable HBV DNA, HBV DNA was cleared more frequently in patients with baseline HBV DNA <2.6 logcopies/ml than in those with baseline HBV DNA ≥4.0 logcopies/ml (100 vs. 50%, $p < .01$) (Table 1).

Serial changes in ALT during lamivudine-to-entecavir switching treatment were further examined. Among the 31 patients with baseline HBV DNA <2.6 logcopies/ml, the baseline ALT was within the normal range (≤40 IU/l) in 27 patients, 24 of whom showed sustained ALT normalization during follow-up. In the remaining three patients, ALT became slightly abnormal (≤60 IU/l) during follow-up. As for four patients with abnormal baseline ALT, the level was normalized in three, whereas a slight elevation of ALT (≤60 IU/l) continued in one during follow-up.

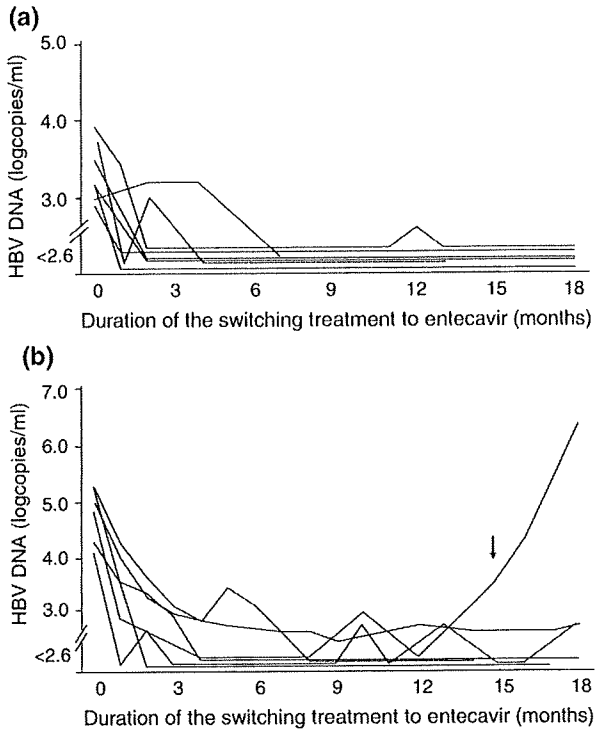

Fig. 1 Changes in HBV DNA after commencement of switching treatment from lamivudine to entecavir in CH-B patients with baseline HBV of (**a**) 2.6–<4.0 logcopies/ml and (**b**) ≥4.0 logcopies/ml. The *black arrow* indicates the time point of virological breakthrough

Among the 13 patients having a detectable level of baseline HBV DNA, five patients (three with baseline HBV DNA of 2.6–<4.0 logcopies/ml and two with baseline HBV DNA ≥4.0 logcopies/ml) had abnormal ALT at baseline but showed ALT normalization during follow-up. In the remaining eight patients, ALT continued to be normal from the beginning of entecavir treatment.

Disease course of the CH-B patients showing entecavir-resistance during lamivudine-to-entecavir switching treatment

The disease course of the entecavir-resistant patient is shown in Fig. 2. This patient was a 33-year-old HBeAg-positive male, whose liver biopsy showed features of chronic hepatitis. He underwent the preceding lamivudine treatment for 8 months. HBV DNA decreased from >7.6 to 4.6 logcopies/ml, and ALT was normalized during the lamivudine therapy. The rtM204V/I substitution was not detected before the switch to entecavir treatment by the PCR–ELMA analysis. After the commencement of entecavir treatment, HBV DNA was cleared at month 5. However, virological breakthrough was seen at month 15, and HBV DNA was further increased to 6.1 logcopies/ml at month 18. The sequencing analysis at month 18 revealed the rtM204V, rtL180M and rtS202G substitutions. Two additional substitutions, rtL267M and rtQ316H, were also found, when the amino acid sequences were compared with three representative genotype C HBV isolates (Genbank accession nos. V00867, X01587 and D00630) [21–23]. Breakthrough hepatitis was not evident after the emergence of entecavir-resistant mutant virus. The sequencing analysis also revealed that he was infected with HBV of genotype C.

Discussion

Entecavir treatment has been shown to exhibit more powerful antiviral efficacy and less frequent drug resistance than lamivudine treatment in nucleos(t)ide analog-naïve CH-B patients [14, 15, 17]. Entecavir is also effective in patients showing lamivudine resistance during the preceding lamivudine treatment, but its efficacy is limited due to the higher incidence of entecavir-resistance, compared with nucleos(t)ide analog-naïve ones [16, 17]. This is because entecavir-resistance is established based on two lamivudine-resistant substitutions, rtM204V and rtL180M, and additional mutation(s) occurring at rt184, rt202 and/or rt250 [18]. A considerable number of CH-B patients remain under continuous lamivudine treatment, while the lamivudine-to-entecavir switching treatment could yield a practical benefit. The switching treatment may be more promising for patients before the appearance of lamivudine resistance than after its development. In the present study, we investigated the efficacy of lamivudine-to-entecavir switching treatment in CH-B patients without apparent evidence of lamivudine resistance during the preceding lamivudine treatment.

We evaluated the antiviral efficacy of the switching treatment to entecavir in relation to the baseline HBV DNA at the commencement of the entecavir administration. In all patients having baseline HBV DNA <2.6 logcopies/ml, who revealed a good response to the preceding lamivudine treatment, HBV DNA continued to be undetectable during the switching treatment to entecavir. Also, all patients having baseline HBV DNA of 2.6–<4.0 logcopies/ml achieved sustained undetectable HBV DNA during the follow-up period of entecavir treatment. Among six patients having baseline HBV DNA ≥4.0 logcopies/ml, who did not respond well to the preceding lamivudine treatment, HBV DNA was cleared in three during follow-up. Its reduction by up to 3.0 logcopies/ml was seen in two additional cases without emergence of the entecavir-resistant virus. Thus, the antiviral efficacy of the lamivudine-to-entecavir switching treatment was exhibited in almost all CH-B patients in parallel with that of the preceding

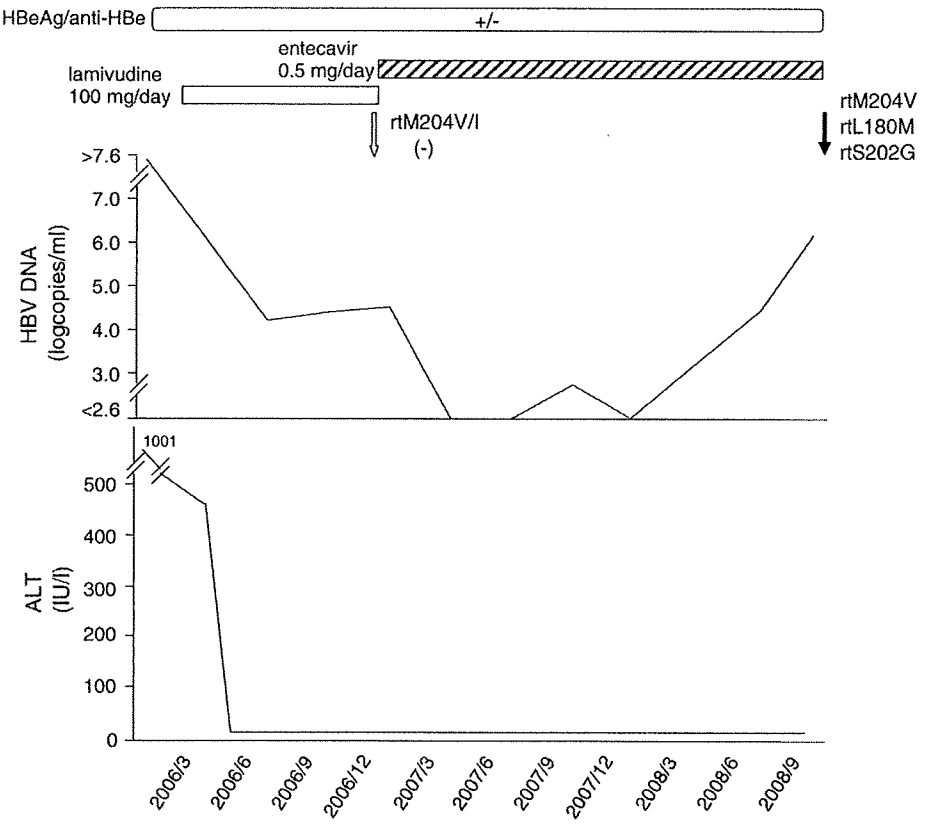

Fig. 2 Disease course of the CH-B patient showing entecavir-resistance during switching treatment to entecavir. The *white arrow* indicates the time point of the PCR–ELMA assay to detect rtM204V/I mutation, whereas the *black arrow* indicates the time point of the PCR-direct sequencing analysis

lamivudine treatment. In addition, the switching treatment to entecavir tended to yield a greater decrease in HBV DNA than the preceding lamivudine treatment. These results indicate that the switch from lamivudine to entecavir may be generally recommendable compared with continuation of lamivudine administration in CH-B patients without evidence of lamivudine resistance.

In this study, one of the six patients having baseline HBV DNA $\geq$4.0 logcopies/ml showed entecavir-resistance during the switching treatment to entecavir. It was probably due to the existence of an extremely small amount of lamivudine-resistant virus mixed with a predominant wild-type virus, which could not be detected by the sensitive PCR–ELMA assay at the start of the switch to entecavir treatment. It is speculated that, during entecavir treatment, the lamivudine-resistant virus having rtM204V and rtL180M substitutions may become predominant with time, followed by the establishment of entecavir-resistant virus via the additional rtS202G substitution. Compared to the low incidence of drug resistance in entecavir treatment for nucleos(t)ide analog-naïve CH-B patients [17], the entecavir-resistance may occur more frequently in the lamivudine-to-entecavir switching treatment for patients without evidence of lamivudine resistance. In particular, patients who do not achieve a good response to the preceding lamivudine treatment are speculated to have a higher risk for the development of entecavir-resistance in the switching treatment to entecavir, although it should be verified by further studies.

In conclusion, in CH-B patients receiving the continuous lamivudine treatment, it may be recommendable to switch to entecavir treatment before the appearance of lamivudine resistance. It may contribute to reducing the subsequent emergence of drug resistance. However, great care should be taken with respect to the emergence of entecavir-resistant virus after the switch to entecavir treatment, especially in patients who do not respond well to the preceding lamivudine treatment. Our retrospective study with a small number of patients and a short duration of follow-up cannot draw a definite conclusion but still provides some information about the clinical possibilities of the lamivudine-to-entecavir switching treatment. Further detailed investigation with a larger number of patients and a longer follow-up period may offer better understanding.

References

1. Lai CL, Chien RN, Leung NW, Chang TT, Guan R, Tai DI, et al. A one-year trial of lamivudine for chronic hepatitis B. Asia Hepatitis Lamivudine Study Group. N Engl J Med. 1998;339:61–8.
2. Dienstag JL, Schiff ER, Wright TL, Perrillo RP, Hann HW, Goodman Z, et al. Lamivudine as initial treatment for chronic

hepatitis B in the United States. N Engl J Med. 1999;341:1256–63.
3. Lai CL, Dienstag J, Schiff E, Leung NW, Atkins M, Hunt C, et al. Prevalence and clinical correlates of YMDD variants during lamivudine therapy for patients with chronic hepatitis B. Clin Infect Dis. 2003;36:687–96.
4. Allen MI, Deslauriers M, Andrews CW, Tipples GA, Walters KA, Tyrrell DL, et al. Identification and characterization of mutations in hepatitis B virus resistant to lamivudine. Lamivudine Clinical Investigation Group. Hepatology. 1998;27:1670–7.
5. Liaw YF, Chien RN, Yeh CT, Tsai SL, Chu CM. Acute exacerbation and hepatitis B virus clearance after emergence of YMDD motif mutation during lamivudine therapy. Hepatology. 1999;30:567–72.
6. Westland CE, Yang H, Delaney WE 4th, Wulfsohn M, Lama N, Gibbs CS, et al. Activity of adefovir dipivoxil against all patterns of lamivudine-resistant hepatitis B viruses in patients. J Viral Hepat. 2005;12:67–73.
7. Ono-Nita SK, Kato N, Shiratori Y, Lan KH, Yoshida H, Carrilho FJ, et al. Susceptibility of lamivudine-resistant hepatitis B virus to other reverse transcriptase inhibitors. J Clin Invest. 1999; 103:1635–40.
8. Hadziyannis SJ, Tassopoulos NC, Heathcote EJ, Chang TT, Kitis G, Rizzetto M, et al. Adefovir dipivoxil for the treatment of hepatitis B e antigen-negative chronic hepatitis B. N Engl J Med. 2003;348:800–7.
9. Marcellin P, Chang TT, Lim SG, Tong MJ, Sievert W, Shiffman ML, et al. Adefovir dipivoxil for the treatment of hepatitis B e antigen-positive chronic hepatitis B. N Engl J Med. 2003; 348:808–16.
10. Perrillo R, Hann HW, Mutimer D, Willems B, Leung N, Lee WM, et al. Adefovir dipivoxil added to ongoing lamivudine in chronic hepatitis B with YMDD mutant hepatitis B virus. Gastroenterology. 2004;126:81–90.
11. Peters MG, Hann Hw H, Martin P, Heathcote EJ, Buggisch P, Rubin R, et al. Adefovir dipivoxil alone or in combination with lamivudine in patients with lamivudine-resistant chronic hepatitis B. Gastroenterology. 2004;126:91–101.
12. van Bömmel F, Wünsche T, Mauss S, Reinke P, Bergk A, Schürmann D, et al. Comparison of adefovir and tenofovir in the treatment of lamivudine-resistant hepatitis B virus infection. Hepatology. 2004;40:1421–5.
13. van Bömmel F, Zöllner B, Sarrazin C, Spengler U, Hüppe D, Möller B, et al. Tenofovir for patients with lamivudine-resistant hepatitis B virus (HBV) infection and high HBV DNA level during adefovir therapy. Hepatology. 2006;44:318–25.
14. Chang TT, Gish RG, de Man R, Gadano A, Sollano J, Chao YC, et al. A comparison of entecavir and lamivudine for HBeAg-positive chronic hepatitis B. N Engl J Med. 2006;354:1001–10.
15. Lai CL, Shouval D, Lok AS, Chang TT, Cheinquer H, Goodman Z, et al. Entecavir versus lamivudine for patients with HBeAg-negative chronic hepatitis B. N Engl J Med. 2006;354:1011–20.
16. Sherman M, Yurdaydin C, Sollano J, Silva M, Liaw YF, Cianciara J, et al. Entecavir for treatment of lamivudine-refractory, HBeAg-positive chronic hepatitis B. Gastroenterology. 2006;130:2039–49.
17. Colonno RJ, Rose R, Pokornowski K, Baldick C, Eggers B, Yu D, et al. Four year assessment of ETV resistance in nucleoside-naïve and lamivudine refractory patients. J Hepatol. 2007; 46:S294. (Abst.).
18. Tenney DJ, Rose RE, Baldick CJ, Levine SM, Pokornowski KA, Walsh AW, et al. Two-year assessment of entecavir resistance in Lamivudine-refractory hepatitis B virus patients reveals different clinical outcomes depending on the resistance substitutions present. Antimicrob Agents Chemother. 2007;51:902–11.
19. Levine S, Hernandez D, Yamanaka G, Zhang S, Rose R, Weinheimer S, et al. Efficacies of entecavir against lamivudine-resistant hepatitis B virus replication and recombinant polymerases in vitro. Antimicrob Agents Chemother. 2002;46:2525–32.
20. Kobayashi S, Ide T, Sata M. Detection of YMDD motif mutations in some lamivudine-untreated asymptomatic hepatitis B virus carriers. J Hepatol. 2001;34:584–6.
21. Ono Y, Onda H, Sasada R, Igarashi K, Sugino Y, Nishioka K. The complete nucleotide sequences of the cloned hepatitis B virus DNA; subtype adr and adw. Nucleic Acids Res. 1983; 11:1747–57.
22. Fujiyama A, Miyanohara A, Nozaki C, Toneyama T, Ohtomo N, Matsubara K. Cloning and structural analyses of hepatitis B DNAs, subtype *adr*. Nucleic Acids Res. 1983;11:4601–10.
23. Kobayashi M, Koike K. Complete nucleotide sequence of hepatitis B virus DNA of subtype adr and its conserved gene organization. Gene. 1984;30:227–32.

Am J Physiol Gastrointest Liver Physiol 296: G157–G167, 2009.
First published December 4, 2008; doi:10.1152/ajpgi.90463.2008.

Transplantation of basic fibroblast growth factor-pretreated adipose tissue-derived stromal cells enhances regression of liver fibrosis in mice

Yoshihiro Kamada, Yuichi Yoshida, Yukiko Saji, Juichi Fukushima, Shinji Tamura, Shinichi Kiso, and Norio Hayashi

Department of Gastroenterology and Hepatology, Osaka University Graduate School of Medicine, Osaka, Japan

Submitted 31 July 2008; accepted in final form 24 November 2008

Kamada Y, Yoshida Y, Saji Y, Fukushima J, Tamura S, Kiso S, Hayashi N. Transplantation of basic fibroblast growth factor-pretreated adipose tissue-derived stromal cells enhances regression of liver fibrosis in mice. *Am J Physiol Gastrointest Liver Physiol* 296: G157–G167, 2009. First published December 4, 2008; doi:10.1152/ajpgi.90463.2008.—Adipose tissue-derived stromal cells (ADSC) potentially differentiate into various cell types similar to bone marrow-derived mesenchymal stromal cells (BMSC). Unlike BMSC, ADSC can be harvested easily and repeatedly. However, the advantages of ADSC for cell transplantation in liver disease remain unclear. To investigate this, we developed a novel culture system for ADSC, as well as effective methods for transplantation of ADSC into mice liver. ADSC were isolated from subcutaneous adipose tissues of male C57BL6/J mice and cultured on plastic dishes with or without basic fibroblast growth factor (bFGF). In the in vivo study, ADSC isolated from green fluorescent protein-transgenic mice were transplanted into carbon tetrachloride-injured C57BL6/J mice liver. bFGF-treated ADSC expressed several liver-specific marker genes and demonstrated liver-related functions such as albumin secretion, glycogen synthesis, urea production, and low-density lipoprotein uptake. Importantly, pretreatment of ADSC with bFGF for 1 wk enhanced the repopulation rate of ADSC in mice liver, attenuated liver fibrosis, and restored normal serum alanine aminotransferase and albumin levels. The results indicate that basic FGF facilitates transdifferentiation of ADSC into hepatic lineage cells in vitro and that transplantation of bFGF-pretreated ADSC reduced hepatic fibrosis in mice. ADSC are a potentially valuable source of cells for transplantation therapy.

hepatic lineage cells; basic FGF; cell transplantation; transdifferentiation; α-smooth muscle actin

LIVER TRANSPLANTATION IS one of the most effective treatments for end-stage liver disease. However, a shortage of suitable donor organs and the requirement for immunosuppression restrict its application. Effective therapies to replace liver transplantation are clearly needed.

Recent studies indicated that bone marrow-derived mesenchymal stromal cells (BMSC) can transdifferentiate into adipogenic, osteogenic, chondrogenic (24), neurogenic (35), myogenic (10), and hepatogenic (18, 23, 26, 28) cells under prescribed conditions. Mesenchymal stromal cells can be isolated from several organs including fetal tissue (6), umbilical cord blood (5), and adipose tissue (37). Adipose-derived stromal cells (ADSC) are similar to BMSC (8, 34), in that both have limited self-renewal ability and can be induced to various mesenchymal tissues and cells including those of hepatic lineage (4, 13, 37). Furthermore, unlike BMSC, ADSC can be repeatedly harvested by a simple and minimally invasive method and can be easily cultured (29). These characteristics are clear advantages of ADSC, making them potentially superior to BMSC as a cell transplantation source.

Basic fibroblast growth factor (bFGF) is essential for initiating liver development (15). We demonstrated previously that bFGF promotes the transdifferentiation of bone marrow cells into hepatic lineage cells in vitro (26). Ishikawa et al. (14) also reported that bFGF facilitates the differentiation of bone marrow cells into hepatic lineage cells in vivo. Thus we reasoned that ADSC could be differentiated into hepatic lineage cells in the presence of bFGF both in vitro and in vivo.

This study developed a primary culture system for mouse ADSC, seeking to differentiate ADSC into hepatic lineage cells in vitro using bFGF. We also investigated the hepatogenic transdifferentiation ability of ADSC in vivo using the carbon tetrachloride (CCl_4)-induced liver-injury mouse model.

MATERIALS AND METHODS

Reagents. Human hepatocyte growth factor (HGF) was provided by Sumitomo Pharmaceuticals (Osaka, Japan). Human bFGF was purchased from Invitrogen (Carlsbad, CA). Human oncostatin M (OSM) was purchased from Genzyme/Techne (Minneapolis, MN). Dimethyl sulfoxide (DMSO) was purchased from Wako Pure Medical (Tokyo, Japan). Knockout serum replacement was purchased from GIBCO-BRL (Grand Island, NY). Primary antibodies were obtained as follows: anti-mouse albumin (goat polyclonal) from Bethyl (Montgomery, TX), anti-human cytokeratin 18 (CK18) (mouse monoclonal) from Sigma (St. Louis, MO), anti-green fluorescent protein (GFP) (rabbit polyclonal) from Medical & Biological Laboratories (Tokyo), anti-alpha smooth muscle actin (α-SMA) (mouse monoclonal) from Dako (Kyoto, Japan), and anti-glyceraldehyde 3-phosphate dehydrogenase (GAPDH) (rabbit polyclonal) from Trevigen (Gaithersburg, MD). Secondary antibodies (Alexa 488-conjugated donkey anti-goat IgG, Alexa 594-conjugated goat anti-rabbit IgG, and Alexa 594-conjugated goat anti-mouse IgG) were purchased from Molecular Probes (Eugene, OR).

Isolation and culturing of ADSC. C57BL/6J mice were purchased from Clea Japan (Tokyo), and the C57BL/6-Tg(CAG-EGFP)C15-001-FJ001Osb mice were kindly provided by Dr. Masaru Okabe (Genome Information Research Center, Osaka University, Osaka, Japan). ADSC were collected from the subcutaneous adipose tissue of 12-wk-old male C57BL/6J mice or C57BL/6-Tg(CAG-EGFP)C15-001-FJ001Osb mice as described previously (21). Briefly, subcutaneous adipose tissues were isolated from mice, minced into fine pieces in phosphate-buffered saline (PBS) containing antibiotic-antimycotic solution (Sigma), and incubated in Dulbecco's modified Eagle's medium (DMEM) containing 1 mg/ml collagenase type II and anti-

Address for reprint requests and other correspondence: S. Kiso, Dept. of Gastroenterology and Hepatology, Osaka Univ., Graduate School of Medicine, 2-2 K1 Yamadaoka, Suita, Osaka 565-0871, Japan (e-mail: kiso@gh.med.osaka-u.ac.jp).

The costs of publication of this article were defrayed in part by the payment of page charges. The article must therefore be hereby marked "*advertisement*" in accordance with 18 U.S.C. Section 1734 solely to indicate this fact.

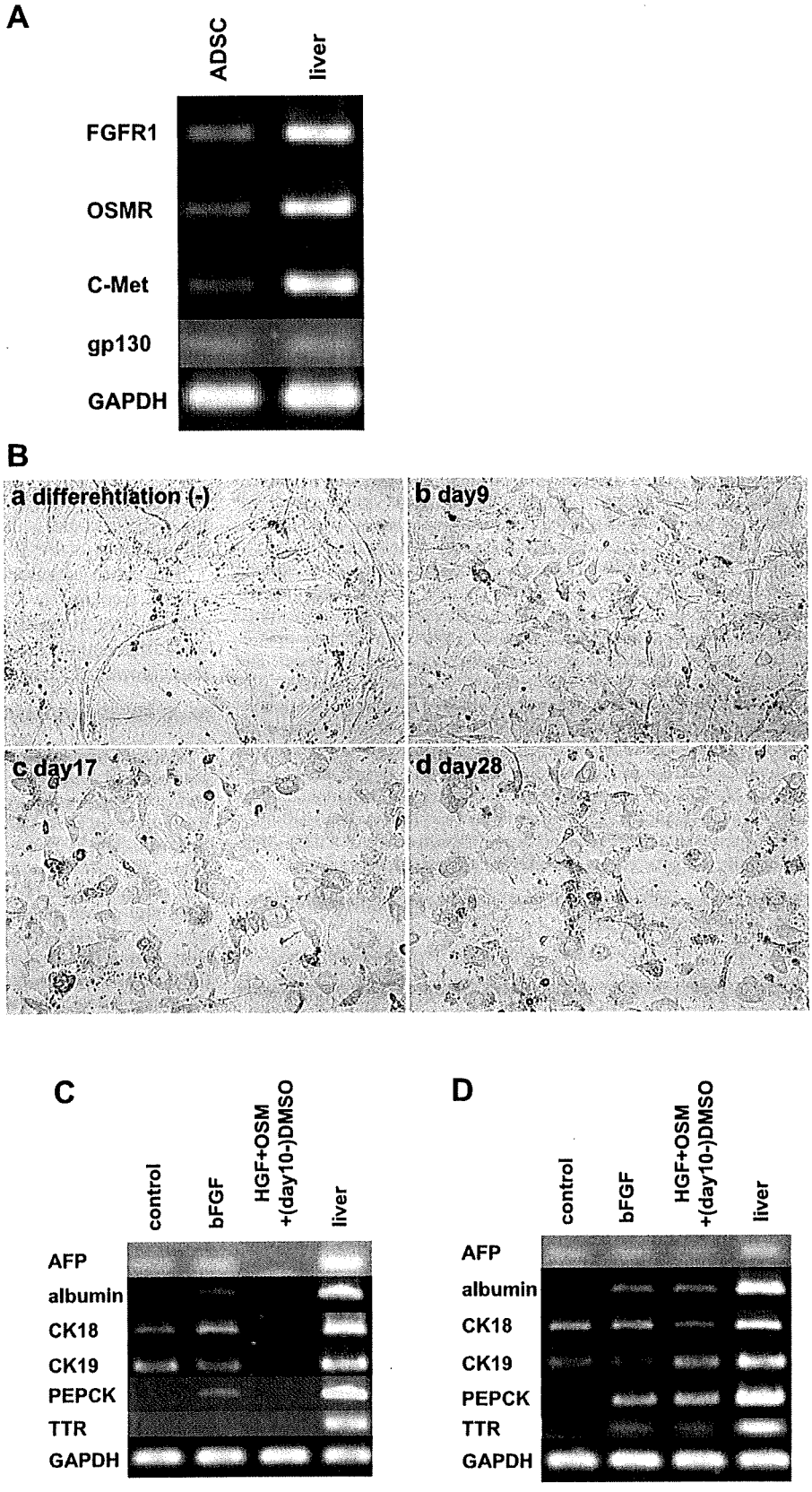

Fig. 1. *A*: expression of growth factor receptor genes in adipose tissue-derived stromal cells (ADSC). RNA was extracted from mouse ADSC (second passages). The mRNA expression levels of FGF receptor-1 (FGFR1), oncostatin M (OSM) receptor (OSMR), c-Met, gp130, and GAPDH were determined by RT-PCR. Mouse liver was used as a positive control. Representative results of 3 experiments with similar findings. *B*: morphological changes in ADSC during differentiation. ADSC were cultured in basic medium containing 20 ng/ml basic FGF (bFGF). Initial fibroblast-like ADSC (*a*) gradually changed to hepatocyte-like polygonal cells at *day 9* (*b*), *day 17* (*c*), and *day 28* (*d*) after differentiation. Original magnification ×100. *C* and *D*: expression of liver-specific genes in ADSC cultured with various growth factors. *C*: ADSC cultured with bFGF for 2 wk expressed alpha fetoprotein (AFP), albumin, cytokeratin 18 (CK18), cytokeratin 19 (CK19), and phosphoenolpyruvate carboxykinase (PEPCK). ADSC cultured with the combination of HGF, OSM, and DMSO for 2 wk showed no hepatocyte-marker gene expression. *D*: ADSC cultured with bFGF for 4 wk expressed albumin, CK18, CK19, PEPCK, and transthyretin (TTR). ADSC cultured with the combination of HGF, OSM, and DMSO for 4 wk also induced hepatocyte-marker gene expression. Representative results of 3 experiments with similar findings.

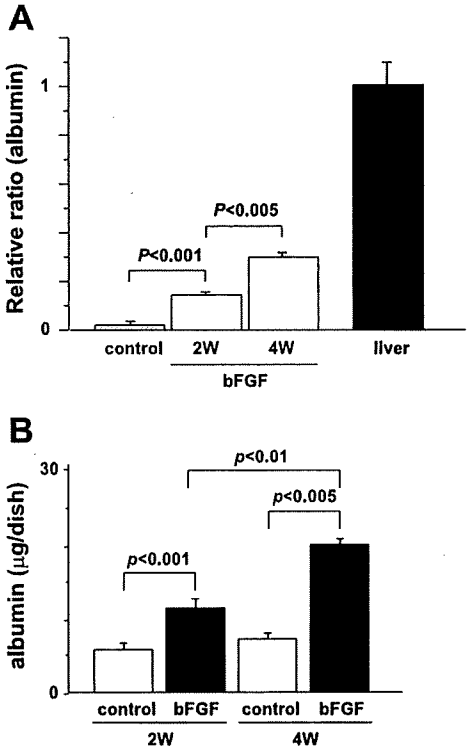

Fig. 2. Quantitative albumin gene expression and albumin synthesis in ADSC. ADSC were cultured on plastic dishes without or with bFGF (20 ng/ml) for 2 or 4 wk (2W and 4W, respectively). *A*: albumin gene expression in ADSC was quantified by real-time PCR. The expression level gradually increased over time in the presence of bFGF. Expression levels in the liver were used as a positive control. Three wells were analyzed for each condition in 2 different experiments. *B*: albumin production by ADSC cultured with bFGF was significantly higher than for control cells (absence of growth factors) ($n = 6$). Three wells were analyzed for each condition in 2 different experiments. Data are means ± SE.

biotic-antimycotic solution at 37°C for 30 min. The tissues digests were filtered thorough sterile 250-μm nylon mesh, centrifuged at 600 *g* for 5 min, and resuspended; this process was repeated twice. ADSC were seeded onto culture dishes with DMEM/10% fetal calf serum (FCS) containing antibiotic-antimycotic solution. In this study, C57BL/6J mice ADSC were used for in vitro studies, and GFP-positive ADSC were used for the in vivo experiments.

Hepatogenic differentiation. ADSC second passages were plated onto plastic dishes in medium (DMEM supplement with 10% Knockout serum replacement, L-glutamine, MEM nonessential amino acids solution, antibiotic-antimycotic solution, and with or without growth factors; 20 ng/ml). The growth factors used were bFGF or the combination of HGF, OSM, and 0.1% DMSO added to the media on the 10th day after differentiation. Culture media were replaced twice a week.

RNA extraction and RT-PCR analysis. Total RNA was extracted from cultured ADSC by using Sepasol-RNA I (nacalai tesque, Osaka, Japan) according to the instructions provided by the manufacturer. RT-PCR was performed using a Gene Amp RNA PCR kit (Applied Biosystems, Branchburg, NJ). PCR conditions were as follows: hot start for 5 min at 95°C, 40 cycles at 95°C for 15 s, 60°C for 15 s, and 72°C for 1 min. The sequences of the primers used in this study are available on request. Real-time PCR was performed on a LightCycler as described previously (16). Primers used in real-time PCR were obtained from Qiagen (Hilden, Germany).

Immunocytochemistry. ADSC were fixed with 4% paraformaldehyde at room temperature for 10 min, followed by incubation with blocking solution comprising PBS and 5% host serum (goat and donkey) for 30 min. The cells were allowed to react with primary antibodies [albumin (1:500), CK18 (1:500)] at room temperature for 1 h and then with secondary antibodies and DAPI (1:5,000) at room temperature for 30 min. Cells were washed with PBS between each step.

Immunohistochemistry and picrosirius red staining. After deparaffinization, the sections were allowed to react with primary antibodies [GFP (1:500), albumin (1:500), α-SMA (1:50)] at room temperature for 1 h and then with secondary antibodies and DAPI at room temperature for 30 min. Specimens were washed with PBS between each step. Picrosirius red (Sigma) staining was used to detect collagen fibrils. The area of fibrosis stained by picrosirius red was quantified by using Adobe Photoshop (Adobe Systems, San Jose, CA).

Immunoblotting. Immunoblotting was performed as described previously (19), using antibodies against α-SMA (1:500 dilution) and GAPDH (1:2,000).

Evaluation of serum ALT and albumin levels. Mice serum alanine aminotransferase (ALT) levels were measured by using a Wako Transaminase CII-Test kit. Serum albumin levels were measured by using an Albumin kit (Wako Pure Medical, Tokyo, Japan), following the protocol supplied by the manufacturer.

Albumin secretion and urea production by ADSC. ADSC were cultured in dishes as described above, in the absence and presence of bFGF. The culture medium was replaced twice a week. Samples of culture supernatants were collected at 2 and 4 wk to measure albumin concentrations by ELISA (Albuwell M, ExoCell, Philadelphia, PA) and urea concentrations by using a Urea assay kit (DIUR-500) according to the instructions supplied by the manufacturer (BioAssay Systems, Hayward, CA). Bovine albumin present in the Knockout serum replacement did not cross-react with the anti-mouse albumin antibody used in the ELISA.

Uptake of LDL. Low-density lipoprotein (LDL) uptake was assessed by incubating cells for 4 h at 37°C with 10 μg/ml Dil-Ac-LDL (Biomedical Technologies, Stoughton, MA). The assay was performed using the method provided by the manufacturer.

Periodic acid-Schiff staining. Cells were fixed with 4% paraformaldehyde for 10 min, and incubated with or without 0.1% α-amylase for 1 h. Then, cells were oxidized in 0.5% periodic acid for 5 min and rinsed twice with water. Cells were then treated with Schiff's reagent for 15 min, rinsed with water, and the nuclei stained with hematoxylin.

Transplantation of GFP-positive ADSC into mice. In this study, 500 μl/kg body wt of CCl_4 was injected intraperitoneally into 8-wk-old recipient male C57BL/6J mice twice a week for 4 wk to induce permanent liver damage. Two days after completion of the CCl_4 treatment, 1×10^5 GFP-positive ADSC second passages pretreated with bFGF (bFGF+ group; $n = 10$) or without bFGF (bFGF− group; $n = 10$) in DMEM/10% FCS containing antibiotic-antimycotic solution for 1 wk were diluted in 100 μl of PBS and then transplanted slowly into mice spleens using a 26-gauge needle. After ADSC injection, the same dose of CCl_4 was continuously injected twice a week to maintain permanent liver damage for 4 more wk. Mice were euthanized 2 days after the final CCl_4 injection, and blood and liver samples were obtained. The liver was either fixed with 4% buffered-paraformaldehyde for histological examination or immediately frozen in liquid nitrogen for RNA extraction. Mice treated with CCl_4 for 8 wk but without transplanted ADSC were used as the CCl_4 control group ($n = 10$). Mice treated with CCl_4 for 4 wk but without ADSC transplantation were used as the 4W group ($n = 4$).

The Ethics Review Committee for Animal Experimentation of Osaka University Graduate School of Medicine approved the study protocol.

Statistical analysis. The results are presented as means ± SE. Differences between groups were examined for statistical significance using analysis of variance with Fisher's paired least significant difference test. Statistical significance was defined as $P < 0.05$.

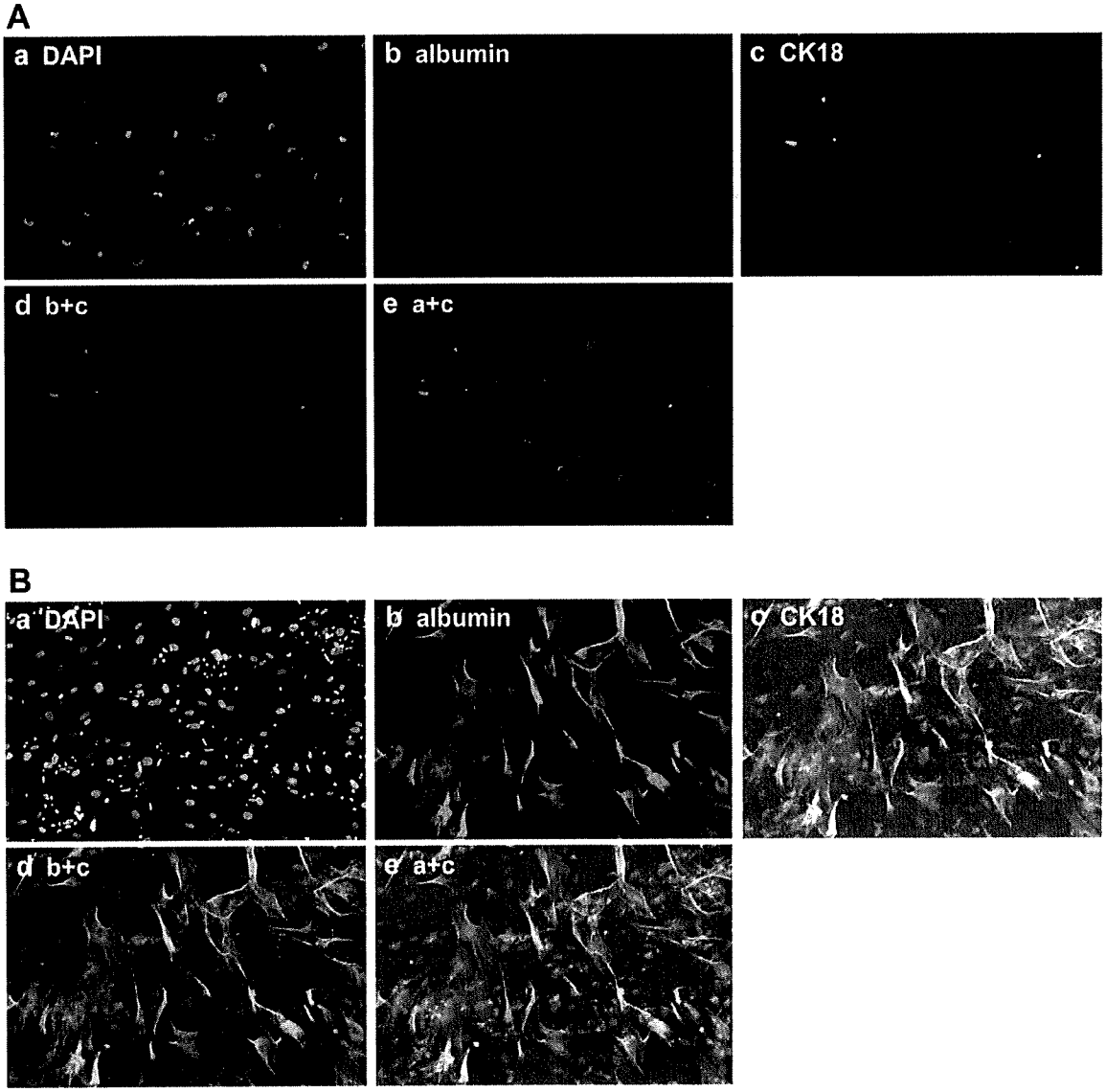

Fig. 3. Immunocytochemistry of albumin and CK18 in bFGF-treated ADSC. ADSC were cultured on plastic dishes without (*A*) or with (*B*) bFGF (20 ng/ml) for 4 wk. Immunofluorescent staining of cultured ADSC for albumin (red) (*b*), CK18 (green) (*c*), and overlap (yellow) (*d*). *a*: Nuclear staining of cultured ADSC with DAPI (blue). *e*: Overlap of *a* and *c*. Original magnification ×200.

RESULTS

Expression of growth factor receptor genes in ADSC. RNA samples were extracted from ADSC cultured in DMEM with 10% FCS. The ADSC showed mRNA expressions of the following: FGF receptor-1 (FGFR1), an FGF-receptor subunit; OSMR, an OSM-receptor subunit; c-Met, an HGF-receptor subunit; and gp130, an OSM-receptor subunit. These results indicated that bFGF, OSM, and HGF can function through these receptors. Mouse liver RNA was used as a positive control (Fig. 1*A*).

ADSC morphology during transdifferentiation into hepatic lineage cells. We next analyzed morphological changes in the ADSC during the differentiation protocol. Undifferentiated ADSC exhibited a fibroblast-like morphology (Fig. 1*Ba*). Culture with 20 ng/ml bFGF produced a gradual change in ADSC morphology from fibroblast-like to hepatocyte-like polygonal cells (Fig. 1*B*, *b–d*).

Liver-specific gene expressions in ADSC cultured with various growth factors. We next assessed the mRNA expression of hepatic-specific markers in ADSC treated with or without growth factors to monitor the hepatic transdifferentiation progress. ADSC cultured with bFGF for 2 wk expressed α-fetoprotein (AFP), albumin, CK18, CK19, and phosphoenolpyruvate carboxykinase (PEPCK) (Fig. 1*C*). In addition, culture in bFGF for 4 wk induced expression of the transthyretin gene, a late-phase hepatic differentiation marker (Fig. 1*D*). ADSC cultured without bFGF (control) expressed CK19 gene, a marker of biliary epithelial cells. However, CK19 gene expression was lower in ADSC treated with

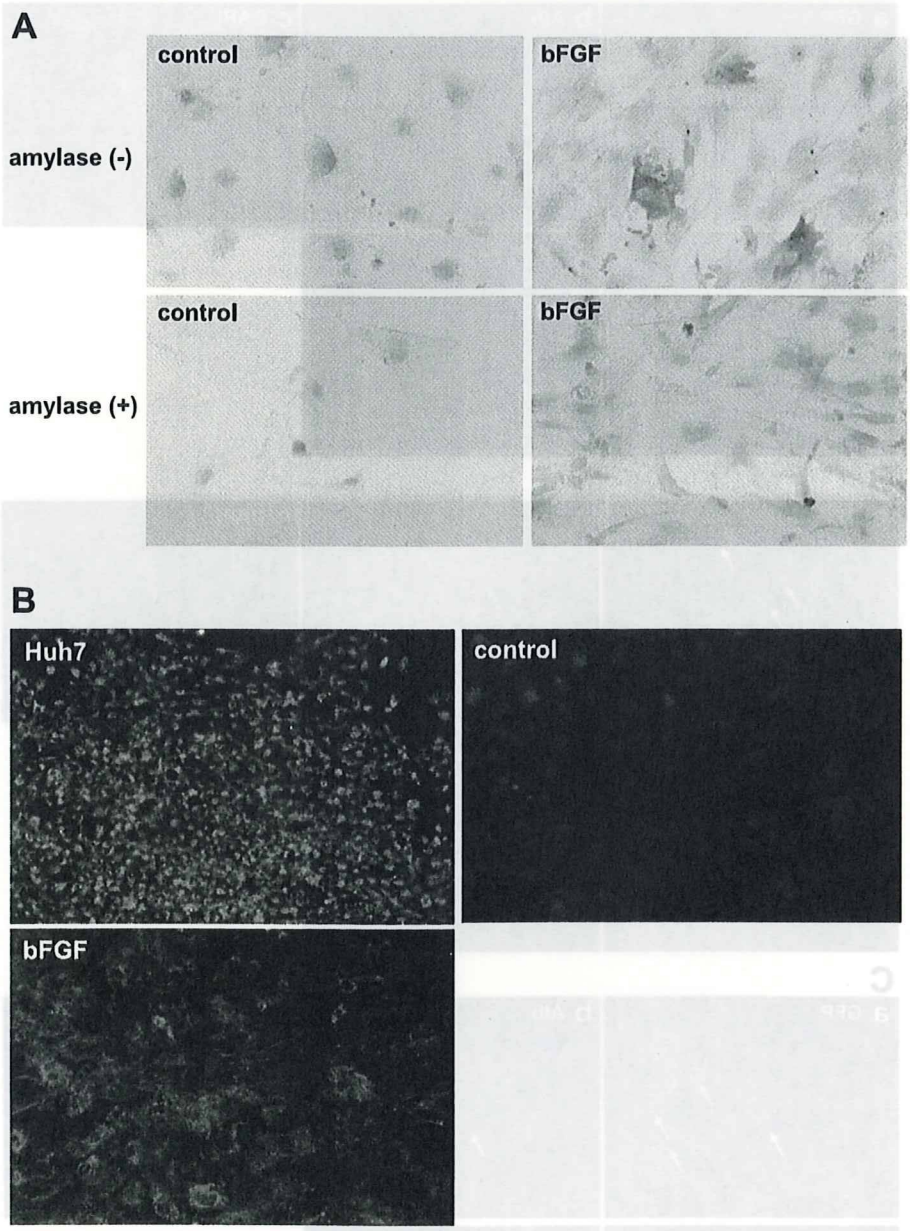

Fig. 4. Hepatocytic function of transdifferentiated ADSC in vitro. ADSC were cultured on plastic dishes without or with bFGF (20 ng/ml). *A*: glycogen-storage capability was assessed by periodic acid-Schiff (PAS) staining in ADSC cultured with bFGF for 4 wk [amylase (−)]. Pretreatment with amylase [amylase (+)] diminished the number of PAS-positive cells. Original magnification ×200. *B*: LDL uptake in ADSC cultured with bFGF for 4 wk and incubated with Dil-Ac-LDL. Huh7 was used as a positive control. Original magnification ×100. *C*: urea production in ADSC cultured with bFGF for 2 or 4 wk. Urea production was assessed by colorimetric assay of the culture supernatants. Data are means ± SE of 6 determinations.

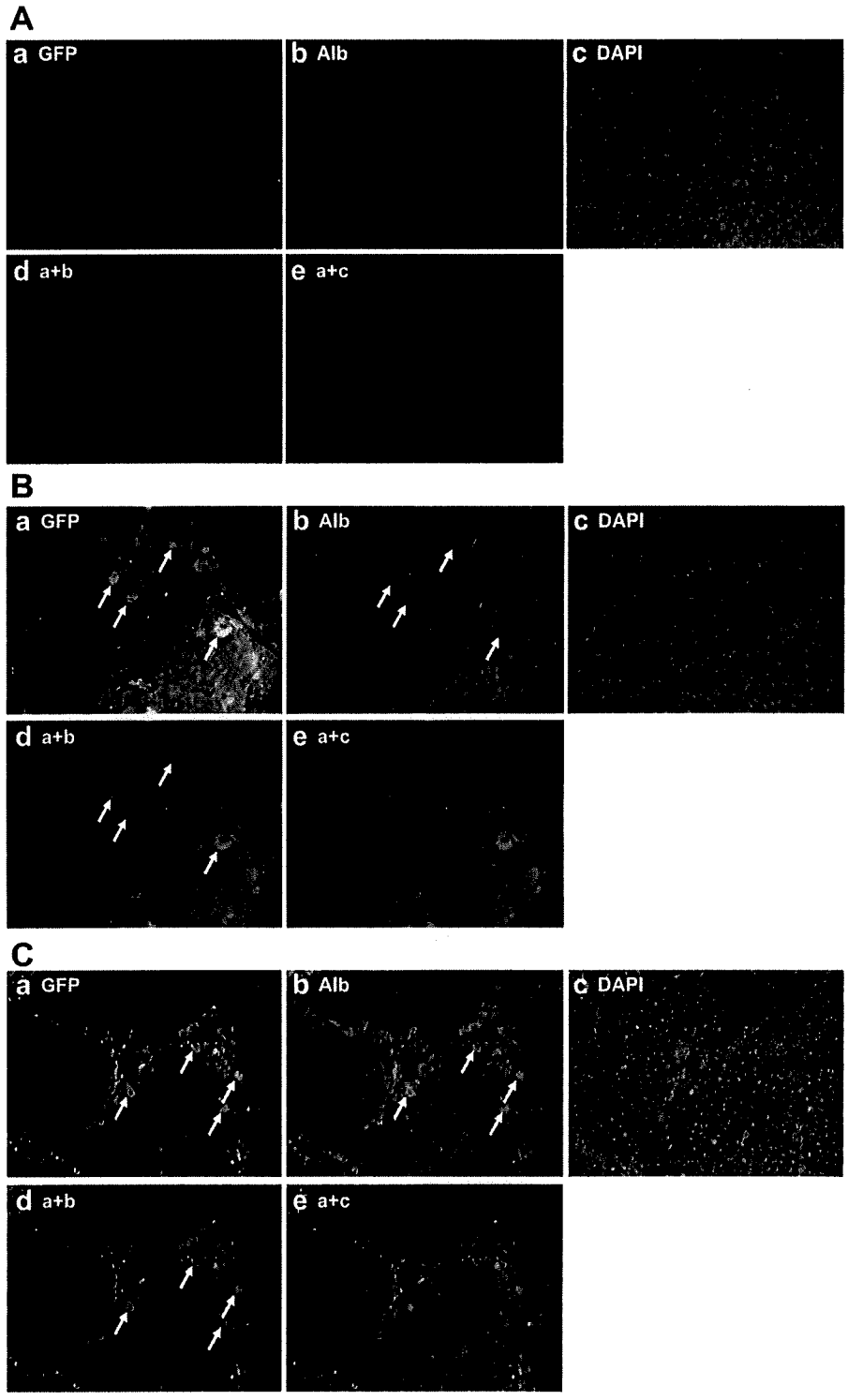

Fig. 5. Immunohistochemistry of ADSC transplanted into CCl_4-injured mice. Mice were injected CCl_4 for 8 wk (500 ml/kg body wt twice weekly). At 4 wk, 1×10^5 green fluorescent protein (GFP)-positive ADSC were injected into the spleen. GFP-positive ADSC were pretreated with bFGF [bFGF+ group; $n = 10$] or without bFGF [bFGF− group; $n = 10$] for 1 wk. Mice treated with CCl_4 and without ADSC injection were used as the CCl_4 group ($n = 10$). Mice were euthanized 2 days after the final CCl_4 injection, and liver samples were obtained. *A*: CCl_4 group. *B*: bFGF− group. *C*: bFGF+ group. *A–C*: immunofluorescence of mice liver with antibodies against GFP (green) (*a*), albumin (Alb; red) (*b*), and overlap (yellow) (*d*) of *a* and *b*. *c*: Nuclear staining of cultured ADSC using DAPI (blue). *e*: Overlap of *a* and *c*. Arrows indicate stained cells. Original magnification ×100.

bFGF for 2 wk and was further reduced in ADSC treated with bFGF for 4 wk (Fig. 1, *C* and *D*). Recently, Seo et al. (31) demonstrated transdifferentiation into hepatogenic cells of human ADSC cultured with the combination of HGF, OSM, and DMSO (31). In our study, mouse ADSC cultured with the same combination also showed hepatocyte-marker gene expression after 4-wk culture, but not after 2-wk culture (Fig. 1, *C* and *D*).

Quantitative albumin gene expression and albumin synthesis by cultured ADSC. Real-time PCR revealed a gradual increase in albumin gene expression in ADSC cultured with bFGF

(Fig. 2*A*). Furthermore, ELISA experiments showed that ADSC cultured in the presence of bFGF secreted significantly higher levels of albumin than cells cultured without bFGF (control) (Fig. 2*B*).

Immunocytochemistry of albumin and CK18 in ADSC treated with bFGF. Analysis of protein expression by immunocytochemistry revealed the expression of albumin and CK18 proteins in ADSC cultured with or without bFGF for 4 wk (Fig. 3). Approximately 25% of the ADSC cultured with bFGF for 4 wk showed positive staining for both albumin and CK18 (Fig. 3*B*), whereas only a few cells were stained for albumin or CK18 in the absence of bFGF (Fig. 3*A*).

Hepatocytic function of transdifferentiated ADSC in vitro. To assess whether hepatic lineage cells derived from ADSC are functionally competent, we analyzed ADSC cultured with or without 20 ng/ml of bFGF for 4 wk. Periodic acid-Schiff staining to reveal glycogen-storage ability showed positive staining in ~5% of ADSC cultured with bFGF, whereas no staining was observed in cells without bFGF (Fig. 4*A*). This positive staining was diminished by amylase pretreatment. These experiments indicated that ADSC cultured with bFGF for 4 wk could store glycogen.

We next examined whether ADSC-derived hepatic lineage cells can uptake LDL by incubating differentiated ADSC with Dil-Ac-LDL. Approximately half the ADSC took up LDL, whereas undifferentiated ADSC did not (Fig. 4*B*). Finally, ADSC-derived hepatic lineage cells were tested for urea production. Undifferentiated ADSC showed no urea production, whereas cells cultured in the presence of bFGF secreted higher amounts of urea in the culture media in a time-dependent manner (Fig. 4*C*).

bFGF facilitated differentiation of transplanted ADSC into hepatic lineage cells. GFP-positive cells were not found in spleens of all mice despite being injected with ADSC (data not shown). A few GFP-positive cells (0.3% of whole cells) were observed in the portal area of the bFGF− group mice livers, whereas none were observed in the CCl_4 group mice livers. However, these GFP-positive cells in ADSC-transplanted mice livers showed only weak albumin protein expression (7.7% of GFP-positive cells) (Fig. 5, *A* and *B*). In contrast, many GFP-positive cells (2.3% of total cells) were observed in the portal area of the bFGF+ group mice livers. Moreover, these GFP-positive cells strongly expressed albumin protein (54.8% of GFP-positive cells) (Fig. 5*C*).

Liver function improves after ADSC transplantation. We compared serum ALT and albumin levels across the three experimental groups. Serum ALT levels were significantly lower in bFGF− mice than in CCl_4-induced mice and tended to be even lower in bFGF+ mice (Fig. 6*A*). Serum albumin levels were significantly elevated in bFGF− mice compared with CCl_4 mice, and interestingly, were further elevated in bFGF+ mice compared with both the CCl_4 and bFGF− groups (Fig. 6*B*).

Transplanted bFGF-pretreated ADSC attenuate liver fibrosis. Liver fibrosis was induced after 8 wk of CCl_4 treatment in mice of the CCl_4 group. ADSC transplantation significantly enhanced this fibrosis in livers of bFGF− mice compared with the CCl_4 group, but liver fibrosis was attenuated in bFGF+ mice livers compared with the other two groups (Fig. 7, *A* and *B*). The severity of liver fibrosis in the bFGF+ group was almost similar to that of the 4W group. This

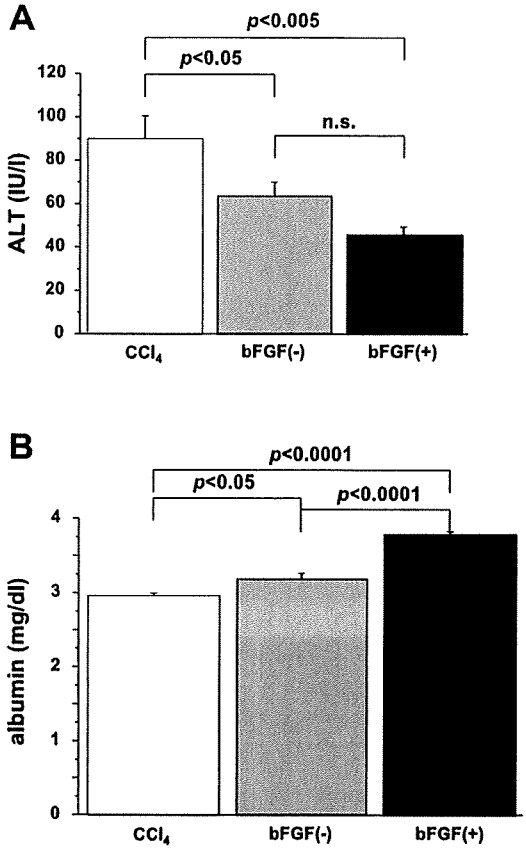

Fig. 6. Serum alanine aminotransferase (ALT) and albumin levels in CCl_4-injured mice with or without ADSC transplantation. Serum ALT (*A*) and serum albumin levels (*B*) for the 3 groups. Mice were euthanized 2 days after the final CCl_4 injection, and blood samples were obtained for measurements of serum ALT and albumin. Data are means ± SE of 10 mice. n.s., Not significant.

indicated that transplantation of bFGF-pretreated ADSC prevented further fibrosis in mice liver. Next, we performed GFP-α-SMA double immunostaining and identified transplanted ADSC-derived myofibroblasts in bFGF− mice livers (Fig. 7*C*). Immunoblotting revealed enhanced α-SMA protein level in bFGF− mice liver (Fig. 7*D*). Moreover, the livers of bFGF+ mice showed low expression levels of fibrogenic markers, transforming growth factor (TGF)-β_1, collagen Iα1, and tissue inhibitor of matrix metalloproteinase 1 (TIMP1), but high expression level of the fibrolytic gene marker matrix metalloproteinase 13 (MMP13) (Fig. 7, *E–H*). The expression levels of collagen Iα1 and TIMP1 were significantly elevated in the liver of bFGF− mice compared with those of CCl_4 mice.

bFGF pretreatment reduces fibrogenic gene expression and increases fibrolytic gene expression in ADSC. Next, we analyzed the expression levels of fibrogenic and fibrolytic genes in ADSC pretreated with or without bFGF. ADSC pretreated with bFGF for 1 wk showed significantly low collagen Iα1 and TIMP1 gene expression levels and increased MMP13 gene expression level compared with untreated ADSC. In addition, a significantly low α-SMA gene expression level was noted in bFGF-pretreated ADSC. However, pretreatment of ADSC with bFGF enhanced TGF-β_1 expression (Fig. 8).

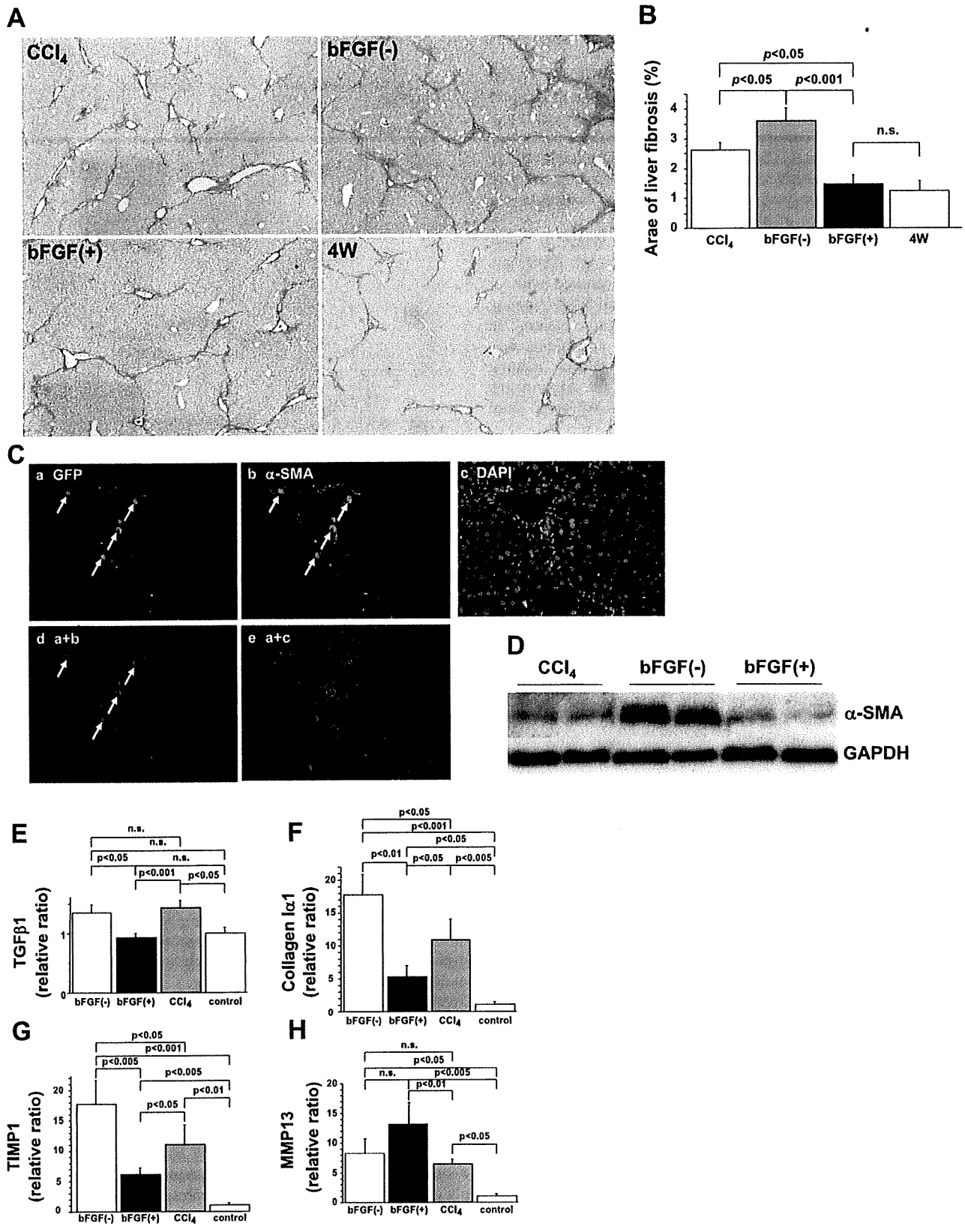

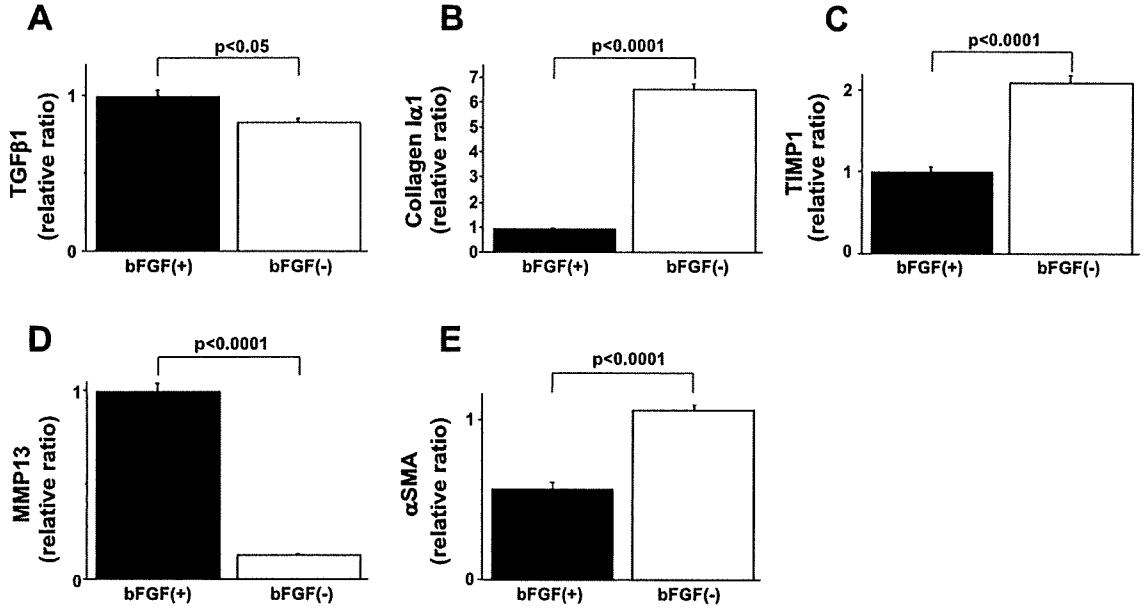

Fig. 8. Expression levels of fibrosis-related genes in ADSC pretreated with or without bFGF. ADSC were cultured on plastic dishes for 1 wk without or with bFGF (20 ng/ml). *A*: TGF-β_1. *B*: collagen Iα1. *C*: TIMP1. *D*: MMP13. *E*: α-SMA. Data are means ± SE (n = 5).

DISCUSSION

The present study demonstrated that bFGF facilitates the transdifferentiation of ADSC into hepatic lineage cells in vitro and in vivo. Unlike BMSC, ADSC can be repeatedly harvested by a simple and minimally invasive method and can be easily cultured (29). These characteristics would make repeated ADSC transplantation easier than BMSC transplantation. Therefore, ADSC represent an equal, if not superior, potential source of undifferentiated cells for liver cell transplantation.

Liver development is a multistep process, mediated by various growth factors and cytokines. At the initial stage of liver development, the foregut endoderm commits to becoming future liver via interactions with the cardiogenic mesoderm. It is at this step that bFGF produced by mesodermal cells participates in hepatic differentiation (15), being required to induce the hepatic fate in the foregut endoderm (30). Previously, we demonstrated that bFGF promotes the transdifferentiation of bone marrow cells into hepatic lineage cells with the induction of transcription factors including hepatocyte nuclear factors and the GATA family of proteins (26). Hepatic expression of FGF genes is upregulated in the CCl_4-induced liver injury mice early after bone marrow transplantation (22). Moreover, pretreatment of bone marrow cells with FGFs, especially bFGF, significantly accelerates the repopulation of bone marrow cells in mice liver (14). The present study demonstrated that bFGF promotes the transdifferentiation of ADSC into hepatic lineage cells both in vitro and in vivo.

Human ADSC were recently reported to transdifferentiate into hepatogenic cells under specific conditions (31). In support of that work, the present study also found that culture of ADSC in media containing HGF and OSM, with 0.1% DMSO added after induction of differentiation, could induce hepatocyte marker genes after 4 wk in culture. However, our cells showed such induction with bFGF at an earlier stage compared with the findings of the other group.

The volume of human bone marrow harvested under local anesthesia is generally limited to 40 ml. This volume contains on average 2.4×10^4 BMSC (3). By contrast, a typical harvest of adipose tissue under local anesthesia can easily exceed 200 ml and contains 1×10^6 ADSC (2). Thus lipoaspirate will yield ~40-fold more stem cells than the equivalent possible harvest of bone marrow (33). Liposuction is one of the most popular cosmetic surgical procedures conducted worldwide (36), raising the possibility of simple and repeatable access to subcutaneous adipose tissue. In addition, ADSC are technically simple to isolate compared with BMSC and exhibit superior features in culture, such as colony frequency and proliferative ability (19).

Unlike BMSC, ADSC express CD34, one of the most well-established stem cell markers (36). After plating, CD34 expression decreased gradually in ADSC, and the expression of mesenchymal stem cell-associated marker, CD105, dramatically increased. These findings confirmed the stem cell capability of ADSC, further enhancing their stature as a cell-source alternative to BMSC.

Fig. 7. Assessment of liver fibrosis in liver of mice with CCl_4 injury. *A*: picrosirius red staining of mice livers after 8 wk (CCl_4, bFGF−, bFGF+) or 4 wk (4W) of CCl_4 treatment. Original magnification ×40. *B*: histographic representation of quantified area of fibrosis area of mice livers. *C*: immunofluorescence of mice liver with antibodies against GFP (green) (*a*), α-smooth muscle actin (α-SMA; red) (*b*), and overlap (yellow) (*d*) of *a* and *b*. *c*: Nuclear staining of cultured ADSC using DAPI (blue). *e*: Overlap of *a* and *c*. Arrows indicate stained cells. Original magnification ×200. *D*: immunoblottings of mice livers. *Top*, α-SMA; *bottom*, GAPDH. The α-SMA protein level was elevated in bFGF− mice livers. Intrahepatic gene expression of TGF-β (*E*), collagen Iα1 (*F*), tissue inhibitor of matrix metalloproteinase 1 (TIMP1; *G*), and matrix metalloproteinase 13 (MMP13; *H*) in the 4 groups. Liver of mice untreated with CCl_4 for 8 wk served as the control. Data are means ± SE of 10 mice.

In our study, transplanted ADSC were successfully engrafted into mice liver and did not disappear after additional 4-wk CCl_4 treatment. GFP-positive transplanted ADSC were still alive and functional 4 wk after final CCl_4 treatment, and the numbers of GFP-positive cells remained almost similar to those at the end of CCl_4 treatment (data not shown). CCl_4 is metabolized into toxic metabolic intermediates through hepatic cytochrome *P*-450 (20). In our in vitro study, ADSC still expressed albumin and CK19 after 4-wk bFGF treatment, indicating that ADSC still possessed the features of both the hepatocyte and biliary epithelial cell after 4-wk bFGF treatment. Although we did not assess the properties of engrafted ADSC in mice liver, it seemed that the transplanted ADSC were still immature and did not express sufficient cytochrome *P*-450 activity at the time of transplantation. In this regard, multipotent stromal cells synthesize a wide variety of growth factors and cytokines, exerting a paracrine effect on local cellular dynamics (7, 11). These bioactive substances might operate in our model, promoting cell survival, and hence improve liver function.

Recent reports claimed that BMSC transplantation attenuates liver fibrosis (12, 27). On the other hand, Russo et al. (25) reported that bone marrow contributed functionally and significantly to liver fibrosis, and they identified bone marrow-derived activated hepatic stellate cells. These results seem contradictory. In the present study, we examined whether ADSC transplantation had a fibrolytic effect on liver fibrosis. ADSC transplantation into our mice significantly enhanced liver fibrosis in bFGF− mice livers compared with the CCl_4 group mice. In contrast, the transplantation of ADSC pretreated with bFGF attenuated liver fibrosis. In addition, bFGF− mice livers contained ADSC-derived α-SMA-positive cells and high hepatic protein level of α-SMA. bFGF stimulates MMP13 at the transcriptional level in human chondrocytes (13), suppresses the promoter activity of collagen I gene in osteoblast-like cells (9), and suppresses TIMP1 gene expression in human periodontal ligament cells (32). In this study, bFGF increased MMP13 expression and decreased the expressions of collagen I and TIMP1 in ADSC. Moreover, we found low protein levels of α-SMA, one of the markers of activated hepatic stellate cells, in bFGF+ mice liver compared with bFGF− mice and found that bFGF decreased α-SMA gene expression in cultured ADSC. bFGF treatment downregulates TGF-β_1-induced α-SMA protein expression in fibroblasts (1, 17). It is possible that this inhibitory effect of bFGF on TGF-β_1 suppresses the activation of hepatic stellate cells. These antifibrotic effects of bFGF on ADSC might therefore reduce the problem of liver fibrosis in cell transplantations.

In conclusion, bFGF induced transdifferentiation of ADSC into hepatic lineage cells both in vitro and in vivo. Moreover, the transplantation of bFGF-pretreated ADSC contributed to the regression of liver function and fibrosis in CCl_4-induced mice liver fibrosis. ADSC can be easily and reproducibly harvested from patients by a simple and minimally invasive method. ADSC-based transplantation for patients with end-stage liver disease could therefore form an important part of therapeutic strategies in this clinical arena.

REFERENCES

1. **Anderson S, DiCesare L, Tan I, Leung T, SundaRaj N.** Rho-mediated assembly of stress fibers is differentially regulated in corneal fibroblasts and myofibroblasts. *Exp Cell Res* 298: 574–583, 2004.
2. **Aust L, Devlin B, Foster SJ, Halvorsen YD, Hicok K, du Laney T, Sen A, Willingmyre GD, Gimble JM.** Yield of human adipose-derived adult stem cells from liposuction aspirates. *Cytotherapy* 6: 7–14, 2004.
3. **Bacigalupo A, Tong J, Podesta M, Piaggio G, Figari O, Colombo P, Sogno G, Tedone E, Moro F, Van Lint MT, Frassoni F, Occhini D, Gualandi F, Lamparelli T, Marmont AM.** Bone marrow harvest for marrow transplantation: effect of multiple small (2 ml) or large (20 ml) aspirates. *Bone Marrow Transplant* 9: 467–470, 1992.
4. **Banas A, Teratani T, Yamamoto Y, Tokuhara M, Takeshita F, Quinn G, Okochi H, Ochiya T.** Adipose tissue-derived mesenchymal stem cells as a source of human hepatocytes. *Hepatology* 46: 219–228, 2007.
5. **Bieback K, Kern S, Kluter H, Eichler H.** Critical parameters for the isolation of mesenchymal stem cells from umbilical cord blood. *Stem Cells* 22: 625–634, 2004.
6. **Campagnoli C, Roberts IA, Kumar S, Bennett PR, Bellantuono I, Fisk NM.** Identification of mesenchymal stem/progenitor cells in human first-trimester fetal blood, liver, and bone marrow. *Blood* 98: 2396–2402, 2001.
7. **Caplan AI, Dennis JE.** Mesenchymal stem cells as trophic mediators. *J Cell Biochem* 98: 1076–1084, 2006.
8. **De Ugarte DA, Morizono K, Elbarbary A, Alfonso Z, Zuk PA, Zhu M, Dragoo JL, Ashjian P, Thomas B, Benhaim P, Chen I, Fraser J, Hedrick MH.** Comparison of multi-lineage cells from human adipose tissue and bone marrow. *Cells Tissues Organs* 174: 101–109, 2003.
9. **Fang MA, Glackin CA, Sadhu A, McDougall S.** Transcriptional regulation of alpha 2(I) collagen gene expression by fibroblast growth factor-2 in MC3T3–E1 osteoblast-like cells. *J Cell Biochem* 80: 550–559, 2001.
10. **Ferrari G, Cusella-DeAngelis G, Coletta M, Paolucci E, Stornaiuolo A, Cossu G, Mavilio F.** Muscle regeneration by bone marrow-derived myogenic progenitors. *Science* 279: 1528–1530, 1998.
11. **Haynesworth SE, Baber MA, Caplan AI.** Cytokine expression by human marrow-derived mesenchymal progenitor cells in vitro: effects of dexamethasone and IL-1 alpha. *J Cell Physiol* 166: 585–592, 1996.
12. **Higashiyama R, Inagaki Y, Hong YY, Kushida M, Nakao S, Niioka M, Watanabe T, Okano H, Matsuzaki Y, Shiota G, Okazaki I.** Bone marrow-derived cells express matrix metalloproteinases and contribute to regression of liver fibrosis in mice. *Hepatology* 45: 213–222, 2007.
13. **Im HJ, Muddasani P, Natarajan V, Schmid TM, Block JA, Davis F, van Wijnen AJ, Loeser RF.** Basic fibroblast growth factor stimulates matrix metalloproteinase-13 via the molecular cross-talk between the mitogen-activated protein kinases and protein kinase Cdelta pathways in human adult articular chondrocytes. *J Biol Chem* 282: 11110–11121, 2007.
14. **Ishikawa T, Terai S, Urata Y, Marumoto Y, Aoyama K, Sakaida I, Murata T, Nishina H, Shinoda K, Uchimura S, Hamamoto Y, Okita K.** Fibroblast growth factor 2 facilitates the differentiation of transplanted bone marrow cells into hepatocytes. *Cell Tissue Res* 323: 221–231, 2006.
15. **Jung J, Zheng M, Goldfarb M, Zaret KS.** Initiation of mammalian liver development from endoderm by fibroblast growth factors. *Science* 284: 1998–2003, 1999.
16. **Kamada Y, Matsumoto H, Tamura S, Fukushima J, Kiso S, Fukui K, Igura T, Maeda N, Kihara S, Funahashi T, Matsuzawa Y, Shimomura I, Hayashi N.** Hypoadiponectinemia accelerates hepatic tumor formation in a nonalcoholic steatohepatitis mouse model. *J Hepatol* 47: 556–564, 2007.
17. **Kawai-Kowase K, Sato H, Oyama Y, Kanai H, Sato M, Doi H, Kurabayashi M.** Basic fibroblast growth factor antagonizes transforming growth factor-b1-induced smooth muscle gene expression through extracellular signal-regulated kinase 1/2 signaling pathway activation. *Arterioscler Thromb Vasc Biol* 24: 1384–1390, 2004.
18. **Lee KD, Kuo TK, Whang-Peng J, Chung YF, Lin CT, Chou SH, Chen JR, Chen YP, Lee OK.** In vitro hepatic differentiation of human mesenchymal stem cells. *Hepatology* 40: 1275–1284, 2004.
19. **Lee RH, Kim B, Choi I, Kim H, Choi HS, Suh K, Bae YC, Jung JS.** Characterization and expression analysis of mesenchymal stem cells from human bone marrow and adipose tissue. *Cell Physiol Biochem* 14: 311–324, 2004.
20. **Masuda Y, Murano T.** Role of cytochrome P-450 in CCl_4-induced microsomal lipid peroxidation. *Biochem Pharmacol* 27: 1983–1985, 1978.
21. **McIntosh M, Hausman D, Martin R, Hausman G.** Dehydroepiandrosterone attenuates preadipocyte growth in primary cultures of stromal-vascular cells. *Am J Physiol Endocrinol Metab* 275: E285–E293, 1998.
22. **Omori K, Terai S, Ishikawa T, Aoyama K, Sakaida I, Nishina H, Shinoda K, Uchimura S, Hamamoto Y, Okita K.** Molecular signature associated with plasticity of bone marrow cell under persistent liver damage by self-organizing-map-based gene expression. *FEBS Lett* 578: 10–20, 2004.

23. **Petersen BE, Bowen WC, Patrene KD, Mars WM, Sullivan AK, Murase N, Boggs SS, Greenberger JS, Goff JP.** Bone marrow as a potential source of hepatic oval cells. *Science* 284: 1168–1170, 1999.
24. **Pittenger MF, Mackay AM, Beck SC, Jaiswal RK, Douglas R, Mosca JD, Moorman MA, Simonetti DW, Craig S, Marshak DR.** Multilineage potential of adult human mesenchymal stem cells. *Science* 284: 143–147, 1999.
25. **Russo FP, Alison MR, Bigger BW, Amofar E, Florou A, Amin F, Bou-Gharios G, Jeffery R, Iredale JP, Forbes SJ.** The bone marrow functionally contributes to liver fibrosis. *Gastroenterology* 130: 1807–1821, 2006.
26. **Saji Y, Tamura S, Yoshida Y, Kiso S, Iizuka AS, Matsumoto H, Kawasaki T, Kamada Y, Matsuzawa Y, Shinomura Y.** Basic fibroblast growth factor promotes the trans-differentiation of mouse bone marrow cells into hepatic lineage cells via multiple liver-enriched transcription factors. *J Hepatol* 41: 545–550, 2004.
27. **Sakaida I, Terai S, Yamamoto N, Aoyama K, Ishikawa T, Nishina H, Okita K.** Transplantation of bone marrow cells reduces CCl4-induced liver fibrosis in mice. *Hepatology* 40: 1304–1311, 2004.
28. **Sato Y, Araki H, Kato J, Nakamura K, Kawano Y, Kobune M, Sato T, Miyanishi K, Takayama T, Takahashi M, Takimoto R, Iyama S, Matsunaga T, Ohtani S, Matsuura A, Hamada H, Niitsu Y.** Human mesenchymal stem cells xenografted directly to rat liver are differentiated into human hepatocytes without fusion. *Blood* 106: 756–763, 2005.
29. **Schaffler A, Buchler C.** Concise review: adipose tissue-derived stromal cells—basic and clinical implications for novel cell-based therapies. *Stem Cells* 25: 818–827, 2007.
30. **Schwartz RE, Reyes M, Koodie L, Jiang Y, Blackstad M, Lund T, Lenvik T, Johnson S, Hu WS, Verfaillie CM.** Multipotent adult progenitor cells from bone marrow differentiate into functional hepatocyte-like cells. *J Clin Invest* 109: 1291–1302, 2002.
31. **Seo MJ, Suh SY, Bae YG, Jung JS.** Differentiation of human adipose stromal cells into hepatic lineage in vitro and in vivo. *Biochem Biophys Res Commun* 328: 258–264, 2005.
32. **Silverio-Ruiz KG, Martinez AE, Garlet GP, Barbosa CF, Silva JS, Cicarelli RM, Valentini SR, Abi-Rached RS, Junior CR.** Opposite effects of bFGF and TGF-beta on collagen metabolism by human periodontal ligament fibroblasts. *Cytokine* 39: 130–137, 2007.
33. **Strem BM, Hicok KC, Zhu M, Wulur I, Alfonso Z, Schreiber RE, Fraser JK, Hedrick MH.** Multipotential differentiation of adipose tissue-derived stem cells. *Keio J Med* 54: 132–141, 2005.
34. **Wagner W, Wein F, Seckinger A, Frankhauser M, Wirkner U, Krause U, Blake J, Schwager C, Eckstein V, Ansorge W, Ho AD.** Comparative characteristics of mesenchymal stem cells from human bone marrow, adipose tissue, and umbilical cord blood. *Exp Hematol* 33: 1402–1416, 2005.
35. **Woodbury D, Schwarz EJ, Prockop DJ, Black B.** Adult rat and human bone marrow stromal cells differentiate into neurons. *J Neurosci Res* 61: 364–370, 2000.
36. **Yoshimura K, Shigeura T, Matsumoto D, Sato T, Takaki Y, Aiba-Kojima E, Sato K, Inoue K, Nagase T, Koshima I, Gonda K.** Characterization of freshly isolated and cultured cells derived from the fatty and fluid portions of liposuction aspirates. *J Cell Physiol* 208: 64–76, 2006.
37. **Zuk PA, Zhu M, Mizuno H, Huang J, Futrell JW, Katz AJ, Benhaim P, Lorenz HP, Hedrick MH.** Multilineage cells from human adipose tissue: implications for cell-based therapies. *Tissue Eng* 7: 211–228, 2001.

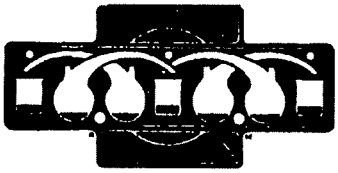

Journal of Viral Hepatitis, 2009, 16, 844–852 doi:10.1111/j.1365-2893.2009.01131.x

Enhanced ability of regulatory T cells in chronic hepatitis C patients with persistently normal alanine aminotransferase levels than those with active hepatitis

I. Itose,[1] T. Kanto,[1] N. Kakita,[1] S. Takebe,[1] M. Inoue,[1] K. Higashitani,[1] M. Miyazaki,[1] H. Miyatake,[1] M. Sakakibara,[1] N. Hiramatsu,[1] T. Takehara,[1] A. Kasahara[2] and N. Hayashi[1]

[1]*Department of Gastroenterology and Hepatology, Osaka University Graduate School of Medicine, Suita, Japan; and* [2]*Department of General Medicine, Osaka University Hospital, Suita, Japan*

Received December 2008; accepted for publication February 2009

SUMMARY. In hepatitis C virus (HCV) infection, the Th1-type immune response is involved in liver injury. A predominance of immunosuppressive regulatory T cells (Treg) is hypothesized in patients with persistently normal alanine aminotransferase (PNALT). Our aim was to clarify the role of Treg in the pathogenesis of PNALT. Fifteen chronically HCV-infected patients with PNALT, 21 with elevated ALT (CH) and 19 healthy subjects (HS) were enrolled. We determined naturally-occurring Treg (N-Treg) as CD4+CD25high+ FOXP3+ T cells. The expression of FOXP3 and CTLA4 in CD4+CD25high+ cells was quantified by real-time reverse transcriptase-polymerase chain reaction. Bulk or CD25-depleted CD4+ T cells cultured with HCV-NS5 loaded dendritic cells were assayed for their proliferation and cytokine release. We examined CD127–CD25–FOXP3+ cells as distinct subsets other than CD25+ N-Treg. The frequencies of N-Treg in patients were significantly higher than those in HS. The FOXP3 and CTLA4 transcripts were higher in PNALT than those in CH. The depletion of CD25+ cells enhanced HCV-specific T cell responses, showing that co-existing CD25+ cells are suppressive. Such inhibitory capacity was more potent in PNALT. The frequency of CD4+CD127–CD25–FOXP3+ cells was higher in CH than those in PNALT. Treg are more abundant in HCV-infected patients, and their suppressor ability is more potent in patients with PNALT than in those with active hepatitis.

Keywords: HCV, PNALT, regulatory T cell.

INTRODUCTION

Hepatitis C virus (HCV) causes a wide range of chronic liver diseases in infected hosts, including chronic hepatitis (CH), liver cirrhosis and hepatocellular carcinoma (HCC). One of the critical determinants promoting the development of HCV-induced liver disease is sustained liver inflammation, explaining the therapeutic rationale of alleviating this condition to help prevent liver cancer [1]. Among chronically infected individuals, approximately 20–30% display persistently normal serum alanine aminotransferase levels [2,3]. Although it is reported that 40–50% of them progress to the active stage of liver inflammation within 5 years of observation [4], the incidence of HCC in the remaining patients continues to be lower than in those with elevated serum ALT levels [5]. Cumulative studies have revealed that HCV is not directly cytopathic to hepatocytes. It has been demonstrated that a Th1-type or cytotoxic T lymphocyte (CTL) response is critically involved in HCV-mediated liver injury [6,7]. Therefore, it is conceivable that some suppressor mechanisms exist against Th1-type immune responses in patients with persistently normal ALT levels (PNALT), which may be distinct from those in patients with active liver inflammation.

Abbreviations: ALT, alanine aminotransferase; CH, chronic hepatitis; CTL, cytotoxic T lymphocyte; DC, dendritic cell; ELISA, enzyme-linked immunosorbent assay; FACS, fluorescence-activated cell sorting; FBS, fetal bovine serum; HBV, hepatitis B virus; HCC, hepatocellular carcinoma; HCV, hepatitis C virus; HS, healthy subjects; IFN, interferon; IL, interleukin; IU, international units; MoDC, monocyte-derived dendritic cell; N-Treg, naturally occurring regulatory T cell; PNALT, persistently normal ALT; RT-PCR, reverse transcriptase-polymerase chain reaction; SLE, systemic lupus erythematosus; TGF, transforming growth factor; Treg, regulatory T cell.

Correspondence: Norio Hayashi, MD, PhD, Department of Gastroenterology and Hepatology, Osaka University Graduate School of Medicine, 2-2 Yamadaoka, Suita, Japan. E-mail: hayashin@gh.med.osaka-u.ac.jp

Regulatory T cells (Treg) are a unique subset of T cells with inhibitory capacity against auto-reactive T cells [8]. Substantial data have been reported about the involvement of Treg in the pathogenesis of various diseases, including autoimmune, cancer or infectious diseases [9–13]. Currently, the existence of several types of Treg has been reported [14]. Naturally occurring Treg (N-Treg) are derived from the thymic stromal environment from progenitor cells and suppress auto-reactive T cells in antigen-specific and antigen-nonspecific manner. Forkhead/winged helix transcription factor (FOXP3) is one of the specific markers of N-Treg, the expression of which is well correlated with the gain of a suppressor function [15,16]. As cells with high expression of CD25 also display FOXP3, it is generally accepted that CD25+FOXP3+ is the most reliable marker for Treg. In HCV infection, several reports have described a higher frequency of N-Treg in the periphery and the liver [17–20], suggesting their active role in HCV persistence. It has also been demonstrated that CD25+FOXP3+ regulatory cells are inducible in the periphery [21]. Owing to the lack of a specific phenotypic marker of these induced regulatory cells, referred to as adaptive Treg, their role in the pathogenesis of HCV infection has not been clearly understood. A recent study has demonstrated that the expression of interleukin (IL)-7 receptor (CD127) is downregulated in Treg to a degree that is inversely correlated with FOXP3 expression [22]. These findings offer the possibility that adaptive Treg are traceable, not all but in part, by the combination of CD127 and FOXP3 independent of CD25 expression.

In this study, our aim was to elucidate whether or not Treg are involved in the pathogenesis of PNALT patients, by comparing the frequency and function of these cell subsets with those in active hepatitis patients or healthy subjects. A distinct equilibrium was found between N-Treg and CD127–CD25–FOXP3+ T cells according to differences in liver inflammation.

MATERIALS AND METHODS

Subjects

Among chronically HCV-infected patients who had been followed at Osaka University Hospital, 15 patients with PNALT levels and 21 patients with elevated or fluctuating ALT levels (the CH group) were enrolled in this study. As controls, 19 healthy subjects (HS) who were negative for HCV and hepatitis B virus (HBV) markers were examined. The study protocol was approved by the ethical committee of Osaka University Graduate School of Medicine. At enrolment, written informed consent was obtained from each subject. In this study, PNALT patients were defined as those whose ALT levels remained within the normal range (<30 IU/mL) without any medications for more than 1 year. At enrolment, the patients were confirmed to be positive for both serum anti-HCV and HCV RNA, but were negative for other viral infections, including HBV and human immunodeficiency virus. The presence of other causes of liver disease, such as autoimmune, alcoholic and metabolic disorders was excluded by the use of laboratory and imaging analyses. Liver biopsy was carried out in some of the patients. Histological examination was performed according to the METAVIR scoring system. In all patients, a combination of repetitive biochemical tests, ultrasonography or computed tomography scans ruled out the presence of cirrhosis and liver tumours. The clinical background of the subjects are shown in Table 1.

Table 1 Baseline clinical characteristics of the patients

	Chronic hepatitis patients	Patients with PNALT	Healthy subjects*	
n	21	15	19	
Sex (M/F)	8/13	5/10	ND	NS
Age	50.6 ± 11.6	47.8 ± 12.7	ND	NS
ALT (IU/L)	88.3 ± 41.4	20.9 ± 6.9	ND	$P < 0.0001^{\dagger}$
Plt ($10^4/\mu L$)	13.5 ± 5.4	20.0 ± 3.9	ND	$P < 0.01^{\dagger}$
HCV RNA (Meq/mL)	8.6 ± 11.3	9.7 ± 7.8	ND	NS

*The background data of healthy subjects (blood donors) were not accessible owing to the confidentiality regulations of the blood centre, but their serum ALT levels were confirmed to be within the normal range. †Statistical significance was analysed by Mann–Whitney *U* test between chronic hepatitis patients and patients with PNALT. The values are expressed as mean ± SD. PNALT, persistently normal alanine aminotransferase level; ND, not determined; NS, not significant; plt, platelet count.

Frequency analyses of Treg cells

For the numerical analyses of Treg cells, heparinized venous blood was obtained from all subjects. Peripheral blood mononuclear cells were collected by density-gradient centrifugation on a Ficoll–Hypaque cushion. The cells were subsequently stained with a combination of various fluorescence-labelled anti-human mouse monoclonal antibodies for phenotypic markers. The antibodies for CD25 (clone B1.49.9) and CD4 (clone 13B8.2) were purchased from Beckman Coulter (Fullerton, CA, USA), that for CD127 (clone 40131) from R&D Systems (Minneapolis, MN, USA) and that for FOXP3-PE (clone PCH101) from eBioscience (San Diego, CA, USA), respectively. The cells were stained in phosphate-buffered saline containing 1% fetal bovine serum (FBS) with various antibodies or isotype controls for 15 min at room temperature. Intracellular staining of FOXP3 was performed using a human FOXP3 staining kit (eBioscience) according to the manufacturer's instructions. The cells were analysed by FACSCalibur (BD Biosciences, San Jose, CA, USA) and CellQuest software.

Functional analysis of CD4+CD25+ T cells in HCV-specific CD4+ T cell response

We first examined the HCV-specific CD4+ T cell response in the presence or absence of CD4+CD25+ T cells. Monocyte-derived dendritic cells (MoDC) were generated from CD14+ cells as reported previously. In brief, CD14+ cells were cultured in Iscove's modified Dulbecco's medium (Gibco Laboratories, Grand Island, NY, USA) supplemented with 10% FBS, 50 IU/mL of penicillin, 50 mg/mL of streptomycin, 2 mM of L-glutamine, 10 mM of Hepes buffer, 10 mM of nonessential amino acids in the presence of 50 ng/mL of granulocyte/macrophage colony-stimulating factor (PeproTech, Rocky Hill, NJ, USA) and 10 ng/mL of IL-4 (PeproTech) for 7 days at 37 °C and 5% CO_2. On day 6 of the culture, MoDC were pulsed with 10 μg/mL of recombinant HCV NS5 (amino acid position: NS5B 1-544; kindly provided by Japan Tobacco, Inc., Tokyo, Japan) and cultured for 24 h. The antigen-pulsed MoDC were then cultured with autologous bulk CD4+ T cells or CD4+CD25– T cells in 96-well flat-bottom plates (Corning, NY, USA) for 5 days. Enrichment of CD4+ T cells or CD4+CD25– T cells was performed using a CD4+CD25+ Regulatory T cell Isolation kit (Miltenyi Biotec, Auburn, CA, USA) according to the manufacturer's instructions. On day 6 of the co-culture, the cells were pulsed with 1 μCi of [3H]-thymidine during the last 16 h of incubation. The supernatants were collected before pulsing with [3H]-thymidine and subjected to cytokine enzyme-linked immunosorbent assay (ELISA). The incorporation of [3H]-thymidine in CD4+ T cells was measured using a β-counter (Wallac-Perkin-Elmer, Wallac, Finland).

Enzyme-linked immunosorbent assay

The concentrations of IL-10, TGF-β1 and interferon (IFN)-γ in the culture supernatants were determined by ELISA. We used matched pairs of relevant monoclonal antibodies (Endogen, Woburn, MA, USA) for IL-10 and IFN-γ, and the DuoSet ELISA development system (R&D Systems) for TGF-β1, according to the manufacturer's instructions. The detection thresholds of IL-10, TGF-β1 and IFN-γ were 10, 10 and 16 pg/mL, respectively.

Real time reverse transcriptase-polymerase chain reaction (RT-PCR)

In order to analyse the expression of FOXP3 and CTLA-4 in N-Treg, we collected CD4+CD25high T cells by using FACSAria. The purity of the isolated cells was more than 95% as determined by FACS. Total RNA was extracted from sorted CD4+CD25high T cells using the RNeasy Mini Kit (Qiagen, Valencia, CA, USA) according to the manufacturer's instructions. Complementary DNA was synthesized using the SuperScript III First-Strand synthesis system (Invitrogen, Carlsbad, CA, USA). Assays-on-demand primers and probes (PE Applied Biosystems, Foster City, CA, USA) were used to quantify FOXP3 and CTLA4 expression. The mRNA levels were evaluated using ABI PRISM 7900 Sequence Detection System (Applied Biosystems). The thermal cycling conditions for all genes were as follows: the reaction was started with a 10-min denaturing cycle at 95 °C, followed by 40 cycles of PCR performed with 15 s of denaturing at 95 °C, then 1 minute at 60 °C for annealing and extension. We identified a calibrator sample from the healthy volunteers. The expressions of molecules were given as the relative values to the calibrator samples. To standardize the amount of total RNA added to each reaction mixture, we quantified β-actin mRNA from each sample as a control of internal RNA and corrected all values with this.

Statistical analysis

Statistical analyses were performed using StatView 5.0 software (SAS Institute Inc., Cary, NC, USA). Mann–Whitney *U*-test was used to compare differences in unpaired samples. For all analyses, a *P*-value of less than 0.05 was considered to be statistically significant.

RESULTS

Peripheral N-Treg are increased in HCV-infected patients

We compared the frequency of Treg between HCV-infected patients and healthy donors. In HCV-positive individuals, they were further categorized into PNALT and CH groups according to the difference in their serum ALT levels. The clinical backgrounds of these groups were not different except for

serum ALT levels and platelet counts (Table 1). N-Treg were defined as the cells with CD4+CD25high+FOXP3+ cells. As the cut-off value between CD25high+ and CD25intermediate+ cells is a critical determinant for Treg analyses, we defined CD4+CD25high+ as the cells with CD25 levels higher than those of CD4–CD25+ cells (Fig. 1a). We first compared the frequency of CD4+FOXP3+ T cells. The frequency of FOXP3+ cells in the CD4+ T cell population in HCV-infected patients was significantly higher than those in the HS (Fig. 1b). However, no difference was observed in FOXP3+ cells between the PNALT and CH patients (Fig. 1b). The frequency of CD4+CD25high+FOXP3+ T cells in CH or PNALT patients were significantly higher than those in HS, whereas those in HCV-positive patients did not differ regardless of their ALT levels (Fig. 1c). Similar results were obtained for the frequency of CD4+CD25–FOXP3+ T cells (Fig. 1d).

Next, we examined whether or not the frequency of N-Treg is correlated with clinical parameters. Among all HCV-infected patients, no correlation was observed between the frequency of N-Treg (CD4+CD25high+ FOXP3+ T cells) and serum ALT, HCV RNA levels, age or platelet counts (data not shown). In the analyses of patients who had undergone liver biopsy, the frequency of N-Treg was not correlated with METAVIR grade/stage scores (data not shown).

The expressions of FOXP3 and CTLA4 are higher in N-Treg from PNALT patients compared with those from the CH group

FOXP3 is the master gene of Treg in the development and gaining of suppressor functions. Alternatively, CTLA4 is one of the key molecules of Treg in exerting inhibitory function. We thus evaluated FOXP3 and CTLA4 mRNA expression in sorted N-Treg (CD4+CD25high+ T cells) by means of real-time RT-PCR. The expression of FOXP3 in PNALT or CH patients was significantly higher than those in HS (Fig. 2a). Of note is the higher expression of FOXP3 in N-Treg from the PNALT group than in those from the CH group (Fig. 2a). In contrast, the expression of CTLA4 in N-Treg from the PNALT was higher than those in the CH, while it did not differ between the CH and HS groups (Fig. 2b).

CD4+CD25+ T cells from PNALT patients have more suppressive capacity in the HCV-specific CD4+ T cell response than those from CH patients

In order to compare the ability of N-Treg to inhibit the antigen-specific CD4+ T cell response, we used autologous MoDC pulsed with HCV proteins as antigen-presenting cells. We examined CD4+ T cell proliferation or cytokine

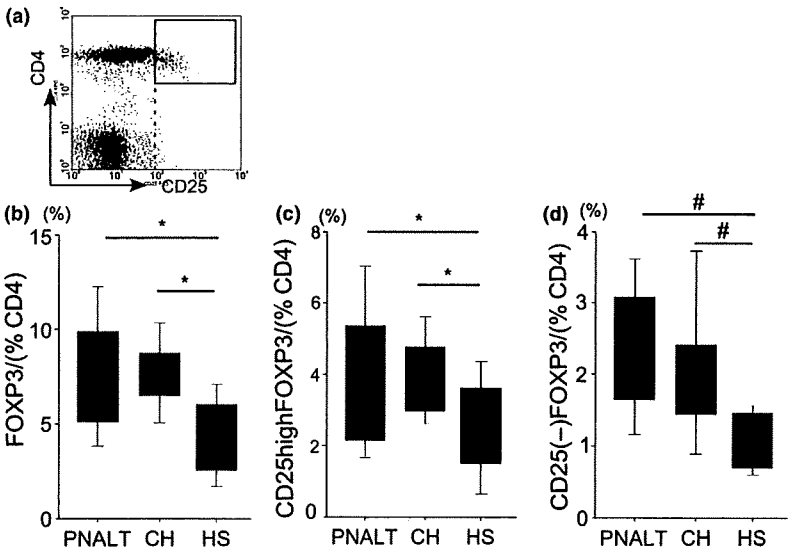

Fig. 1 Comparison of frequencies of naturally-occurring regulatory T cells (N-Treg) and FOXP3-positive cells among the groups. (a) Gating of CD4+CD25high+ T cells under FACS analysis. The cut-off value of CD25high expression is set at a level that is more than that of CD4–CD25+ cells (dotted line); CD4+CD25high+ T cells are shown in the rectangle drawn in the representative dot plot. (b) Frequencies of FOXP3+ cells, (c) N-Treg (CD25high+FOXP3+ cells) and (d) CD25–FOXP3+ cells in CD4+ T cells were compared among the groups. Boxes represent lower and upper quartiles with the median value (solid line) between boxes, while the whiskers represent the minimum and maximum values. *, $P < 0.05$; , $P < 0.0001$ by Mann–Whitney *U*-test. *Abbreviations:* PNALT, hepatitis C virus (HCV)-infected patients with persistently normal alanine aminotransferase (ALT) levels; CH, HCV-infected patients with elevated ALT levels; HS, healthy subjects.